

# Hole Pinning Clearance

Fritz Scholz\*

Research and Technology  
Boeing Information & Support Services

## Abstract

Two parts, each with two holes, are to be pinned together by some type of fastener. Nominally the holes on part 1 are to match the holes on part 2 and the fastener diameters should be smaller than the hole diameters. Due to variation in hole diameters, fastener diameters and hole center positions loose pinning of the two parts may no longer be possible. The problem considered here is to define a pinning criterion which, when nonpositive, expresses by how much we may have missed loose pinning, and which, when positive indicates the amount of slack left over after pinning. The problem is first reduced to a one-dimensional one by aligning the parts on the axes connecting the actual hole centers on each part. The proposed criterion is the maximum of the minimum plays at the two matched hole pairs. By play is meant the difference between the diameter of the biggest circle fitting inside an (overlapping) hole pair and the corresponding fastener diameter. The criterion is definitely nonlinear and traditional RSS methodology is inappropriate here. Worst case and statistical tolerancing are examined under the special scenario that a) the nominal hole diameters are the same with diameter variations governed by a common uniform distribution, b) the nominal fastener diameters are the same with diameter variations governed by a common uniform distribution, and c) the nominal hole centers are matched for the two parts with variation governed by a common circular symmetric, bivariate normal distribution. The hole diameters on the same part are modeled to be identical. An example calculation shows that under worst case tolerancing the required nominal hole clearance is over 100% larger than under statistical tolerancing.

Further, the effect of deviations from perpendicularity of the hole center axes is examined. Depending on the part thickness such deviations will reduce the effective diameter of the hole. This effective diameter is the largest diameter of a cylinder that will pass through the hole in perpendicular fashion. Deviations from perpendicularity are again modeled by a circular symmetric, bivariate normal distribution for the location  $(X, Y)$  of the hole center exit location projected onto the entry plane. Again an example calculation is given. Tables are provided for easy use of the statistical tolerancing methods.

---

\*P.O. Box 3707, MS 7L-22, Seattle WA 98124-2207, e-mail: fritz.scholz@boeing.com

# Hole Pinning Clearance

## 1 Problem Description

The diagram in Figure 1 shows two parts to be pinned by two bolts, rivets, or expanding temporary fasteners, referred to as pins from now on. At issue is whether the variations in the hole diameters  $D_1, \dots, D_4$ , hole center locations, and minimum fastener diameters  $d_1, d_2$  allow successful loose pinning of the two parts. The distance from hole center 1 to hole center 2 is denoted by  $X_1$  and the distance from hole center 3 to hole center 4 is denoted by  $X_2$ . Here the holes are referenced by the same indices as the corresponding hole diameters. Furthermore, it is assumed that the axis connecting hole centers 1 and 2 is aligned with the axis connecting hole centers 3 and 4. Such alignment will give the best opportunity for pinning and thus reduces the problem to a one-dimensional one along that alignment axis. All motions of part 2, referred to below, will be along this axis.

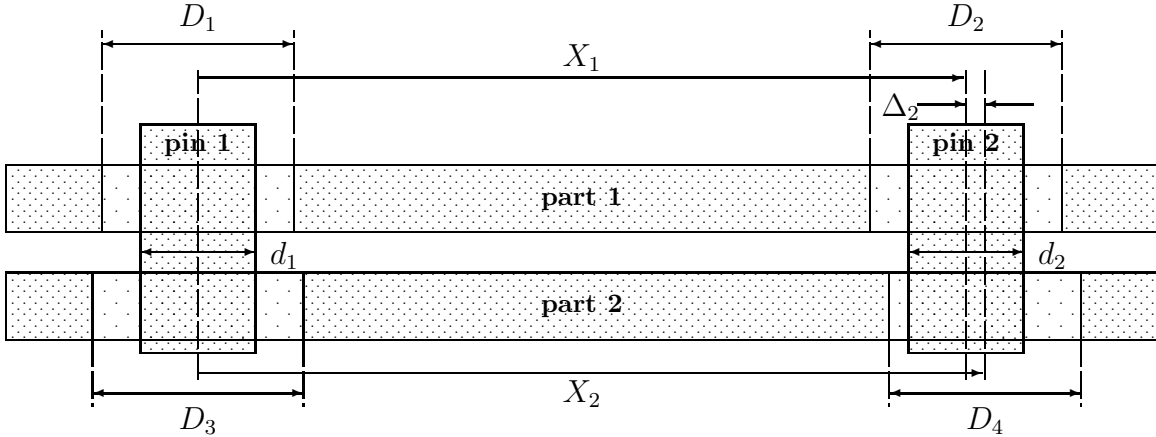


Figure 1. Pinning of two hole pairs

As shown in Figure 1, hole centers 1 and 3 are aligned, allowing for a maximum clearance diameter of  $\min(D_1, D_3)$  for pin 1. The hole centers 2 and 4 are therefore misaligned by the amount  $\Delta_2$ . In Figure 1 we have  $\Delta_2 = |X_1 - X_2|$ , because of the alignment at the centers 1 and 3. However, the largest diameter of a pin that can pass through holes 2 and 4 depends only on the misalignment distance  $\Delta_2$ , and on  $D_2$  and  $D_4$ , regardless of whether holes 1 and 3 are aligned or not. In fact, that clearance diameter for pin 2 is

$$Q_2(\Delta_2) = \min \left( D_2, D_4, \frac{D_2}{2} + \frac{D_4}{2} - \Delta_2 \right),$$

where  $\Delta_2$  does not necessarily have to equal  $|X_1 - X_2|$ . Here  $(D_2 + D_4)/2 - \Delta_2$  could theoretically be negative, but typically it should be unlikely. A negative clearance diameter indicates no clearance and says how far away one may be from any positive clearance.

The above expression for  $Q_2(\Delta_2)$  can be seen by distinguishing the following two cases. Either one hole of the holes 2 and 4 is contained within the other, in which case the clearance diameter is  $\min(D_2, D_4)$ , or the two holes overlap. In that latter case the clearance diameter is  $(D_2 + D_4)/2 - \Delta_2$ , as is seen quite easily from Figure 1.

In a symmetrical fashion the clearance diameter at holes 1 and 3, when their hole centers have distance  $\Delta_1$ , is given by

$$Q_1(\Delta_1) = \min \left( D_1, D_3, \frac{D_1}{2} + \frac{D_3}{2} - \Delta_1 \right) .$$

In order to determine whether two such parts can be loosely pinned it would be useful to develop a criterion that measures the slack or play left after pinning. Positive slack would mean that the parts can be pinned and more easily so for larger slack. For nonpositive slack loose pinning would not be possible. It is not immediately obvious how to define such a measure of slack. We assume that pins 1 and 2 should not be interchangeable, i.e., pin 1 will have to go through holes 1 and 3 and pin 2 will have to go through holes 2 and 4.

So far there have been no constraints on the dimensions  $D_i$ ,  $d_i$  and the hole centers. Presumably the distances between the nominal hole centers should be equal. Also, the nominal value for  $d_1$  should be smaller than the smaller of the nominal values for  $D_1$  and  $D_3$ , with similar relations holding between the nominals of  $d_2$ ,  $D_2$ , and  $D_4$ . In most situations one may take the nominals for  $D_1, \dots, D_4$  to be the same and also the nominals for  $d_1$  and  $d_2$  to be equal. However, it is conceivable that  $D_3$  and  $D_4$  are significantly larger than the counterparts  $D_1$  and  $D_2$ . This could come about either through excessive variation or differences in nominals for the  $D_i$ 's. Furthermore, the pin diameters  $d_1$  and  $d_2$  may barely clear  $D_1$  and  $D_2$ , respectively. In that case one may have significant motion slack between parts 1 and 2, but one barely is able to get the pins through holes 1 and 2. The question is: Which of these two aspects matters with regard to the ability to pin this assembly?

## 2 Pinning Criterion

We propose the following approach. For any given position of the parts, aligned along the hole center axes, one can determine by the above clearance diameters which of the two pins will have less play, i.e., we can determine the minimum play for this position. By “play” we mean the difference between maximum allowed pin diameter at that hole pair and in that position and the actual pin diameter. Such play, if positive, allows us to move the loose pin back and forth within the hole pair. As we move the parts relative to each other along the alignment axis we affect this minimum play at the two hole pairs. The criterion we propose is the maximum of the minimum plays one can achieve with such part motions.

When holes 1 and 3 are aligned on their centers, then pin 1 has the maximum play it will ever get, namely  $\min(D_1, D_3) - d_1$ . At the same time pin 2 has play  $Q_2(|X_1 - X_2|) - d_2$ .

Thus the minimum play at this position is

$$P_1 = \min [\min(D_1, D_3) - d_1, Q_2(|X_1 - X_2|) - d_2] .$$

On the other hand, when holes 2 and 4 are aligned on their centers, then pin 2 has the maximum play it will ever get, namely  $\min(D_2, D_4) - d_2$ . At the same time pin 1 has play  $Q_1(|X_1 - X_2|) - d_1$ . Thus the minimum play at this position is

$$P_2 = \min [\min(D_2, D_4) - d_2, Q_1(|X_1 - X_2|) - d_1] .$$

Of these two minimum plays,  $P_1$  and  $P_2$ , one is typically the larger, but the question is: Can one find a position with even larger play? Usually the answer is yes and in Appendix A it is shown that  $P_{\max-\min}$  can be expressed as follows

$$\begin{aligned} P_{\max-\min} = & \frac{|D_1 - D_3| + |D_2 - D_4|}{4} + \frac{\min(D_1, D_3) + \min(D_2, D_4)}{2} - \frac{d_1 + d_2}{2} \\ & - \frac{1}{2} \max \left( |X_1 - X_2|, \frac{|D_1 - D_3| + |D_2 - D_4|}{2} \right. \\ & \left. + |\min(D_1, D_3) - d_1 - [\min(D_2, D_4) - d_2]| \right) . \end{aligned} \quad (1)$$

Note that the form of this expression is hardly a linear stack of dimensions nor is it approximately linearizable because of the absolute value and minimum functions. The absolute value function  $f(x) = |x|$  cannot be approximated well by a linear function near  $x = 0$  and the  $\min(x, y)$  function suffers similarly for  $x \approx y$ , since

$$\min(x, y) = \frac{x + y}{2} - \frac{|x - y|}{2} , \quad (2)$$

which is valid for all  $x$  and  $y$ .

### 3 Worst Case Tolerancing

Here we will consider worst case tolerancing in a special, yet important case. Namely, we assume that the nominals and tolerances for the  $D_i$  are all the same, and similarly for the  $d_i$ , i.e., we assume  $a \leq D_i \leq b$  for  $i = 1, 2, 3, 4$ ,  $c \leq d_i \leq d$  for  $i = 1, 2$ . Furthermore, concerning the hole center locations we assume that they are within  $r$  of the nominal centers and it is assumed that the nominal centers for paired holes match. Through a series of steps we find the smallest value for  $P_{\max-\min}$ , i.e., the worst case that is possible under the above tolerance constraints.

As a preliminary consideration note that under the above hole centering tolerance assumptions it follows that the maximal allowed value of  $|X_1 - X_2|$  is  $4r$ . This value can be

achieved when the holes on one part are as close together as possible while on the other part they are as far apart as possible.

Considering the form of  $P_{\max-\min}$  given in (1) for fixed  $D_i$  and  $d_i$  and for variable  $|X_1 - X_2|$  we see that  $P_{\max-\min}$  is nonincreasing in  $|X_1 - X_2|$ . Thus  $P_{\max-\min}$  is smallest when  $|X_1 - X_2|$  is as large as allowed, namely  $4r$ .

Next, keeping  $|X_1 - X_2| = 4r$  and holding  $\min(D_1, D_3) = D_1^*$ ,  $\min(D_2, D_4) = D_2^*$ ,  $d_1, d_2$  fixed, while varying  $|D_1 - D_3|$  and  $|D_2 - D_4|$  we see that  $P_{\max-\min}$  remains either constant or decreases as  $|D_1 - D_3|$  and  $|D_2 - D_4|$  decrease. It follows that the lowest value for  $P_{\max-\min}$  is achieved by setting  $|D_1 - D_3| = 0$  and  $|D_2 - D_4| = 0$ .

After the above minimizing steps the problem has been reduced to minimizing

$$P_{\max-\min} = \frac{D_1 - d_1 + D_2 - d_2}{2} - \frac{1}{2} \max(4r, |D_1 - d_1 - (D_2 - d_2)|)$$

over  $d_i \in [c, d]$  and  $D_i \in [a, b]$ . For  $|D_1 - d_1 - (D_2 - d_2)| \leq 4r$  that minimum value is  $a - d - 2r$  and is attained when  $D_i = a$ ,  $d_i = d$  for  $i = 1, 2$ . For  $|D_1 - d_1 - (D_2 - d_2)| > 4r$  that minimum value can be at most (using identity (2))

$$\min(D_1 - d_1, D_2 - d_2) \geq a - d$$

which is greater than in the previous case. Thus the absolute attainable minimum for  $P_{\max-\min}$  is  $a - d - 2r$ . This is intuitively quite obvious and on that basis could have been arrived at more directly. Namely, mismatch the hole centers as much as possible and make hole diameters as small as possible and pin diameters as large as possible (i.e. go for maximum material condition in each case).

In order to guarantee loose pinning for all parts satisfying the given tolerances we have to have  $a - d - 2r > 0$ .

## 4 Statistical Tolerancing

Under the statistical tolerancing view of the same problem one would treat the variation of the dimensions  $|X_1 - X_2|$ ,  $D_1, \dots, D_4$ , and  $d_1, d_2$  as random, varying mostly independently of each other according to some distribution. The proper choice of distribution in each case is not always obvious, especially in the absence of process control data. The assumptions made below can be challenged and changed, but the basic approach to finding the distribution of  $P_{\max-\min}$  would remain the same. Here we are no longer interested in the worst (smallest) possible value for  $P_{\max-\min}$  but in its distribution as induced by the variations in  $|X_1 - X_2|$ ,  $D_1, \dots, D_4$ , and  $d_1, d_2$ . From this distribution we can derive the probability for positive play at both hole pairs, i.e.,

$$p = P(P_{\max-\min} > 0) .$$

If  $p < 1$ , we have a positive chance of no loose pinning. For small  $1 - p$  this may well be acceptable in view of other benefits gained, e.g., relaxed part tolerance requirements.

It was noted above that the expression (1) for  $P_{\max-\min}$  is not linearizable. Thus the traditional RSS methodology is not appropriate here. In principle, given the nature of the part

variations, it should be possible to develop the distribution of  $P_{\max-\min}$ , either analytically or by simulation. Even when an analytical approach may be possible, it will usually still be extremely messy.

#### 4.1 Modeling Part Variation

We now discuss the assumptions made for the variation of parts. First, we assume that the hole centers vary according to a circular symmetric, bivariate normal distribution around the respective nominals, which are supposed to be identical for matched pairs. Denoting the  $i^{\text{th}}$  hole center location by  $(U_i, V_i)$  with nominal  $(\mu_i, \nu_i)$ , where

$$(\mu_1, \nu_1) = (\mu_3, \nu_3) \quad \text{and} \quad (\mu_2, \nu_2) = (\mu_4, \nu_4),$$

we note that circular bivariate normality means that the  $U_i, V_i$  are all independent with common standard deviation  $\sigma$ , where  $\sigma$  controls the variation of the hole centers around the respective nominals. For example, if the hole centering accuracy is specified by

$$\gamma = P\left(\sqrt{(U_1 - \mu_1)^2 + (V_1 - \nu_1)^2} \leq r\right) = 1 - \exp\left(-\frac{r^2}{2\sigma^2}\right)$$

then  $r$  relates to  $\gamma$  and  $\sigma$  as follows

$$r = \sigma \sqrt{-2 \log_e(1 - \gamma)} \tag{3}$$

which for  $\gamma = .9973$  results in  $r = 3.4394\sigma$ . We can express the absolute hole center distance mismatch  $|X_1 - X_2|$  as follows using  $\mathbf{U} = (U_1, U_2, U_3, U_4)$  and  $\mathbf{V} = (V_1, V_2, V_3, V_4)$

$$\begin{aligned} |X_1 - X_2| &= \left| \sqrt{(U_1 - U_2)^2 + (V_1 - V_2)^2} - \sqrt{(U_3 - U_4)^2 + (V_3 - V_4)^2} \right| \\ &= |f(\mathbf{U}, \mathbf{V})|, \quad \text{with} \quad f(\mathbf{U}, \mathbf{V}) = X_1 - X_2 \end{aligned}$$

and observe that under our assumptions the two square root expressions are independent and have the same distribution, namely

$$\sqrt{(U_1 - U_2)^2 + (V_1 - V_2)^2} = \sigma\sqrt{2} G_{2,\delta}$$

where the random variable  $G_{2,\delta}$  has a noncentral chi-distribution with 2 degrees of freedom and with non-centrality parameter  $\delta = \ell^2/(2\sigma^2)$ . Here  $\ell$  denotes the common nominal distance between the hole center pairs, i.e.,

$$\ell = \sqrt{(\mu_1 - \mu_2)^2 + (\nu_1 - \nu_2)^2} = \sqrt{(\mu_3 - \mu_4)^2 + (\nu_3 - \nu_4)^2}.$$

Thus the difference of these square roots, i.e.,  $X_1 - X_2$ , will have a distribution symmetric around zero, but not necessarily normal. However, since  $\ell$  is typically much larger than  $\sigma$ , usually by orders of magnitude, one can linearize the expression for  $X_1 - X_2$  quite well

using a one term Taylor expansion of  $f(\mathbf{U}, \mathbf{V})$  around  $(\boldsymbol{\mu}, \boldsymbol{\nu})$  with  $\boldsymbol{\mu} = (\nu_1, \dots, \nu_4)$  and  $\boldsymbol{\nu} = (\nu_1, \dots, \nu_4)$ , namely

$$\begin{aligned}
f(\mathbf{U}, \mathbf{V}) &\approx f(\boldsymbol{\mu}, \boldsymbol{\nu}) + \frac{\mu_1 - \mu_2}{\ell} [U_1 - \mu_1 - (U_2 - \mu_2) - (U_3 - \mu_3) + (U_4 - \mu_4)] \\
&\quad + \frac{\nu_1 - \nu_2}{\ell} [V_1 - \nu_1 - (V_2 - \nu_2) - (V_3 - \nu_3) + (V_4 - \nu_4)] \\
&= \frac{\mu_1 - \mu_2}{\ell} [U_1 - \mu_1 - (U_2 - \mu_2) - (U_3 - \mu_3) + (U_4 - \mu_4)] \\
&\quad + \frac{\nu_1 - \nu_2}{\ell} [V_1 - \nu_1 - (V_2 - \nu_2) - (V_3 - \nu_3) + (V_4 - \nu_4)] \\
&\sim \mathcal{N}\left(0, \left[\frac{(\mu_1 - \mu_2)^2}{\ell^2} + \frac{(\nu_1 - \nu_2)^2}{\ell^2}\right] 4\sigma^2\right) = \mathcal{N}\left(0, (2\sigma)^2\right).
\end{aligned}$$

Thus the linearized approximation of  $X_1 - X_2$  has a normal distribution with mean zero and standard deviation  $2\sigma$ . The quality of this approximation is illustrated in Figure 2. There 10,000 simulations of the actual values of  $X_1 - X_2$  were generated, using  $\sigma = 1$  and four different values for  $\ell$ , namely  $\ell = 0, 2, 5, 20$ . The histograms in the left column of Figure 2 summarize these simulations. Superimposed in each case is the normal distribution resulting from the linearization, with mean zero and standard deviation  $2\sigma = 2$ . Note that for  $\ell \geq 5\sigma$  the approximation is quite good. The cases with  $\ell = 0$  and  $\ell = 2\sigma$  are actually of little interest, since the two hole pairs would never be drilled in such close proximity where they almost coincide. These two cases are only given to show that the linearization approximation can break down. The distribution of the absolute difference  $|X_1 - X_2|$  will be quite skewed. This is illustrated in the right column of Figure 2. However, from our previous approximation discussion it is clear that we can approximate these distributions for  $\ell \geq 5\sigma$  quite well by the distribution of the absolute value of a normal random variable with mean zero and standard deviation  $2\sigma$ . These approximations are again shown superimposed on the histograms on the right side of Figure 2.

Above we assumed a circular symmetric, bivariate normal distribution for  $(U_i, V_i)$  around the nominal hole centers  $(\mu_i, \nu_i)$ . Often the hole centering process is biased, i.e., consistently off target by the same bias vector. For holes drilled under simple translation on the same part, i.e., without rotation of the axis connecting the two nominal hole centers relative to the bias vector, such bias would be the same and thus the loose pinning issue would not be affected, although the position of the pinned parts relative to each other would be changed by such a bias vector.

For the common distribution of  $D_1, \dots, D_4$  we could use a normal distribution, centered over the interval  $[a, b]$  and containing 99.73% of that distribution in that interval. A more realistic assumption is that the distributions be uniform over the range  $[a, b]$ . This seems to reflect tool wear more accurately and it is the assumption with which we will proceed.

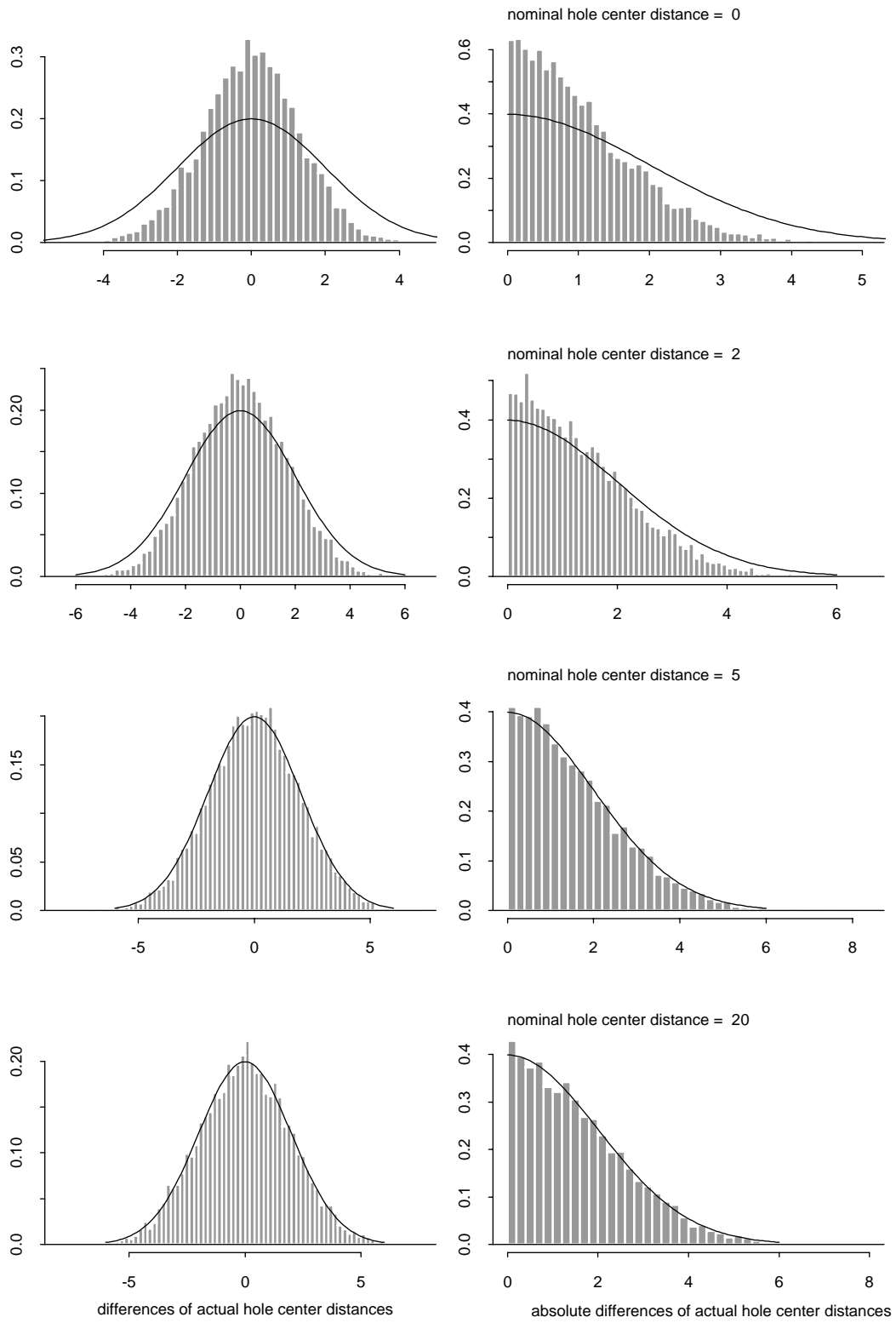


Figure 2. Simulated hole center distance mismatches for two hole pairs



It would seem that holes on the same part have hole diameters which are more or less the same, since they were presumably drilled in succession. Thus we should not treat  $D_1$  and  $D_2$  as independent, but instead use  $D_1 = D_2$  in our modeling. Similarly we proceed with  $D_3$  and  $D_4$ . However, the pairs  $(D_1, D_2)$  and  $(D_3, D_4)$  may well be considered as independent of each other, unless indicated to the contrary by other information concerning the part manufacture.

The diameters  $d_1, d_2$  of the pins we will treat as independently varying according to a uniform distribution over the range  $[c, d]$ . This again assumes that tool wear in producing the fasteners is the major driver in the pin diameter variation. However here it seems reasonable to assume that pins have been mixed sufficiently so that the pin diameter variation is independent from pin to pin. Of course, it is possible that pins manufactured in close succession have been kept paired for some reason, but we assume that this is not the case.

## 4.2 Distribution of $P_{\max-\min}$

Under the above assumptions on part variation, in particular using  $D_1 = D_2$  and  $D_3 = D_4$ , the form of  $P_{\max-\min}$  further simplifies to

$$\begin{aligned} P_{\max-\min} &= \frac{|D_1 - D_3|}{2} + \min(D_1, D_3) - \frac{d_1 + d_2}{2} \\ &\quad - \frac{1}{2} \max(|X_1 - X_2|, |D_1 - D_3| + |d_1 - d_2|) \\ &= \frac{D_1 + D_3}{2} - \frac{d_1 + d_2}{2} - \frac{1}{2} \max(|X_1 - X_2|, |D_1 - D_3| + |d_1 - d_2|) \end{aligned}$$

where again the identity (2) was used. Even in this simplified form an analytical solution for the distribution of  $P_{\max-\min}$  appears to be very difficult to obtain. One component of  $P_{\max-\min}$ , namely the difference

$$\frac{D_1 + D_3}{2} - \frac{d_1 + d_2}{2}$$

varies around the nominal hole to pin clearance

$$\eta = \frac{a + b}{2} - \frac{c + d}{2} = D_0 - d_0 ,$$

where  $D_0 = (a + b)/2$  is the nominal hole diameter and  $d_0 = (c + d)/2$  is the nominal pin diameter. However,  $P_{\max-\min}$  is reduced consistently by the remaining component, namely by the positive random variable

$$\frac{1}{2} \max(|X_1 - X_2|, |D_1 - D_3| + |d_1 - d_2|) .$$

In understanding the variation of  $P_{\max-\min}$  it simplifies matters to standardize it as follows

$$\frac{P_{\max-\min} - \eta}{r} = \frac{D_1 + D_3 - (a + b)}{2r} - \frac{d_1 + d_2 - (c + d)}{2r}$$

$$-\frac{1}{2} \max \left( \frac{|X_1 - X_2|}{r}, \frac{|D_1 - D_3| + |d_1 - d_2|}{r} \right).$$

Note that the distributions of the terms on the right depend only on the two parameters  $\rho_1 = (b - a)/r$  and  $\rho_2 = (d - c)/r$ , since

$$\frac{D_i - D_0}{r} = \frac{D_i - (a + b)/2}{r} = \frac{1}{2} \frac{D_i - (a + b)/2}{(b - a)/2} \frac{b - a}{r} \sim V_i \frac{b - a}{r} = \rho_1 V_i$$

and

$$\frac{d_i - d_0}{r} = \frac{d_i - (c + d)/2}{r} = \frac{1}{2} \frac{d_i - (c + d)/2}{(d - c)/2} \frac{d - c}{r} \sim \tilde{V}_i \frac{d - c}{r} = \rho_2 \tilde{V}_i$$

with  $V_i$  and  $\tilde{V}_i$  independent and uniformly distributed over the interval  $[-\frac{1}{2}, \frac{1}{2}]$ , and

$$\frac{X_1 - X_2}{r} = \frac{X_1 - X_2}{2\sigma} \frac{2\sigma}{r} = Z \frac{2\sigma}{r}$$

has the same distribution as  $(2/3.4394) Z = .5815 Z$ , where  $Z$  is a standard normal random variable. Here we used the relation  $r = 3.4394\sigma$  from (3) with  $\gamma = .9973$ .

Using this notation we find that  $(P_{\max-\min} - \eta)/r$  has the same distribution as

$$T = \frac{1}{2} (V_1 + V_3) \rho_1 - \frac{1}{2} (\tilde{V}_1 + \tilde{V}_2) \rho_2 - \frac{1}{2} \max \left( .5815 |Z|, |V_1 - V_3| \rho_1 + |\tilde{V}_1 - \tilde{V}_2| \rho_2 \right).$$

The distribution of  $T$  can be simulated for various values of  $(\rho_1, \rho_2)$ . Equivalently this can be done for various values of  $(\rho, \kappa)$  with  $\rho = \rho_1$  and  $\kappa = \rho_2/\rho_1$ . Such simulated distributions can then be compared against the corresponding standardized worst case value, namely

$$\frac{1}{r} \left[ a - d - 2r - \left( \frac{a + b}{2} - \frac{c + d}{2} \right) \right] = -2 - \frac{1}{2}(\rho_1 + \rho_2).$$

Figure 3 shows the histograms for four sets of 100,000 such simulations of  $T$ , using  $\kappa = 1$  and  $\rho = .2, .5, 1, 2$ , i.e.,  $\rho_1 = \rho_2 = .2, .5, 1, 2$ . The lowest 10 values of  $T$  are shown as individual tickmarks below the histogram, since they are not represented well by the latter.

Note that these distributions do not look normal, which is further confirmation that ordinary RSS tolerancing is not appropriate here. RSS tolerancing is based on approximately linear tolerance stacking which also entails approximate normality for the tolerance stack via the central limit theorem.

There appears to be a fair amount of separation between the lower ends of the simulated distributions and the respective standardized worst case values. One may make use of this gap by relaxing some or all of the tolerances that one has some control over or one may want to reduce the nominal hole to pin clearance  $\eta$  in order to reduce undesirable slack after loose pinning. In taking either of these measures one may even want to disregard the 10 low (or more) tickmark values, since they represent  $1/10000^{\text{th}}$  of all simulated cases. Such a

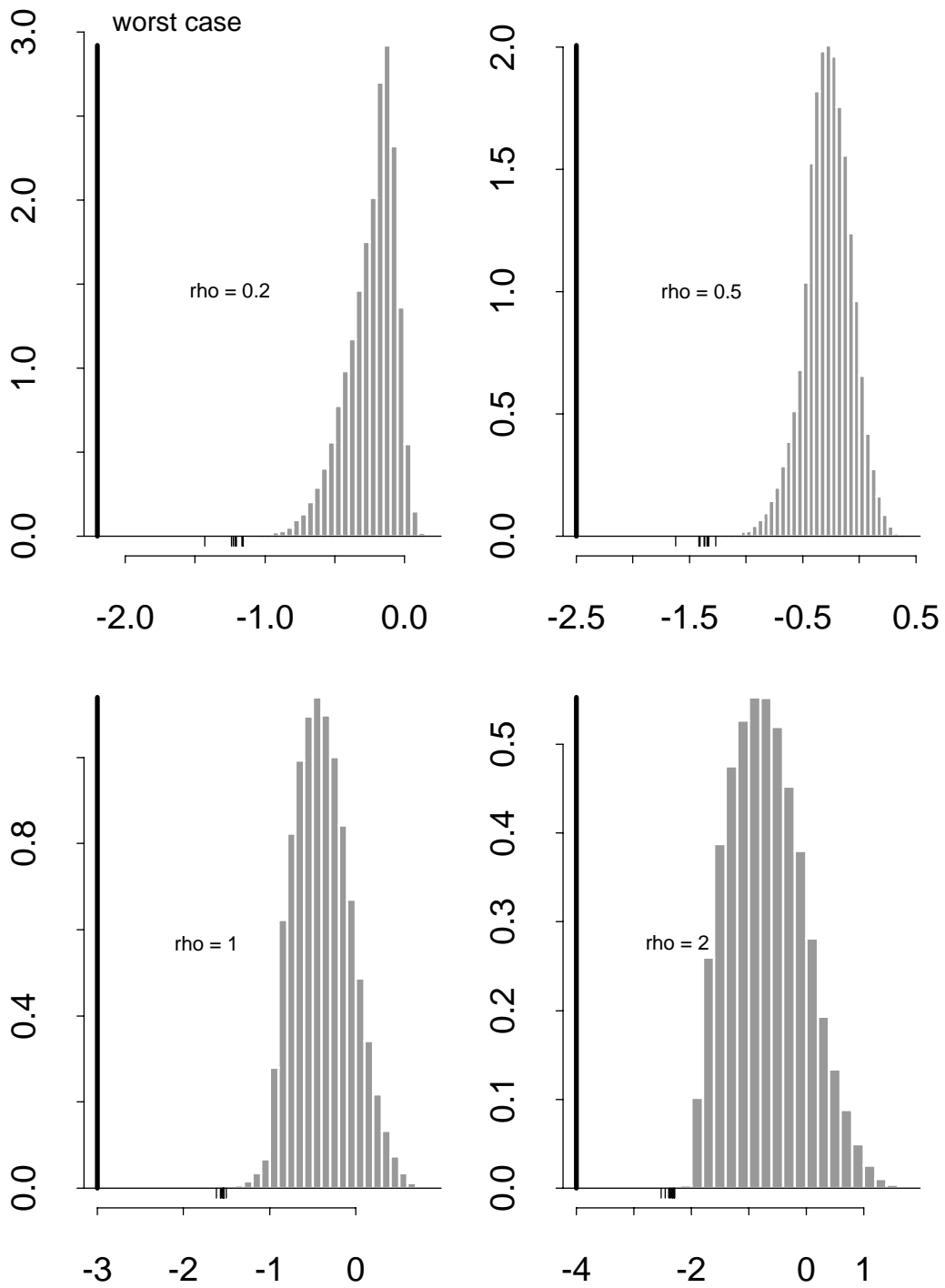


Figure 3. Simulated distributions of  $T$ , for  $\kappa = 1$ ,  $\rho = 1, 2, 3, 4$ , and 100,000 simulations

defect rate for the inability to pin loosely may outweigh the corresponding gains in tolerance relaxation.

In using these results systematically, with proper accounting of the risks involved, it is best to find various low quantiles  $t_p$  of  $T$ , where  $t_p$  is defined by

$$P(T \leq t_p) = p.$$

Of interest here are the  $t_p$  values for very small  $p$ , such as  $p = .001$  or  $p = .0001$ . Since we do not know the exact distribution of  $T$ , we can only estimate the  $t_p$  by the corresponding sample quantiles  $\hat{t}_p$ , which are loosely defined by

$$p = \frac{\#\{T_i \leq \hat{t}_p, i = 1, \dots, N\}}{N}$$

where  $N = 100,000$  is the number of simulated  $T_i$  values and  $\#\{T_i \leq \hat{t}_p, i = 1, \dots, N\}$  is the number of  $T_i$  which are  $\leq \hat{t}_p$ .

When plotting  $\hat{t}_p$  against  $-\log_{10}(p)$  for small  $p$  one finds an almost linear pattern. See Figure 4, which shows the estimated quantiles in relation the corresponding the  $-\log_{10}(p)$  values for  $\kappa = 1$  and  $\rho = .1, .3, .5, .75, .9, 1, 1.1, 1.2, 1.3, 1.4, 1.6, 1.8, 1.9, 2, (.25), 5$ , each based on an independent set of 100,000 simulations. The fluctuations in the  $\hat{t}_p$  values are due to simulation variation in the tails of the distribution, which gets more pronounced the further out one goes, i.e., for smaller  $p$  values. We summarize the  $-\log_{10}(p)$  to  $\hat{t}_p$  relationship by fitting a straight line via ordinary least squares.

These fitted lines vary in slope and intercept with  $\rho$ . The intercepts decrease significantly with increasing  $\rho$ , whereas the slopes show a less straightforward pattern. Both patterns with superimposed spline curves are shown in Figure 5 for the lines fitted in Figure 4. Since these point patterns still show considerable roughness they were replicated 10 times, with each  $\rho$  value on each replication giving rise to 100,000 simulations. The intercepts and slopes from these 10 replications were averaged and are shown in Figures 6-7 together with superimposed smoothing spline curves. For  $\rho_1 = \rho_2 = \rho$ , Figures 6-7 may be used to read off appropriate intercept and slope values  $\alpha(\rho)$  and  $\beta(\rho)$ . Then, for given risk  $p$  of no loose pinning, proceed to calculate

$$\hat{t}_p(\rho) = \alpha(\rho) + \beta(\rho) [-\log_{10}(p)]$$

and thus we have (subject to a small simulation error) that the maximal minimum play  $P_{\max-\min}$  exceeds

$$m_0 = \eta + r \hat{t}_p(\rho) = \frac{a + b - c - d}{2} + r \hat{t}_p(\rho)$$

with probability  $1 - p$ . Typically one would make this minimum value either  $m_0 = 0$  or  $m_0 = \epsilon$  where  $\epsilon > 0$  is some small positive number that represents a subjective safe margin deemed necessary to avoid binding while inserting the pins.

Covering a reasonably wide range of  $\kappa = \rho_2/\rho_1$ , similar simulations were run for  $\kappa = .1, 1/3, .5, 2/3$ . The corresponding Figures are given in Appendix C. The intercept and slope coefficients are presented in a more compact form in Table 1.

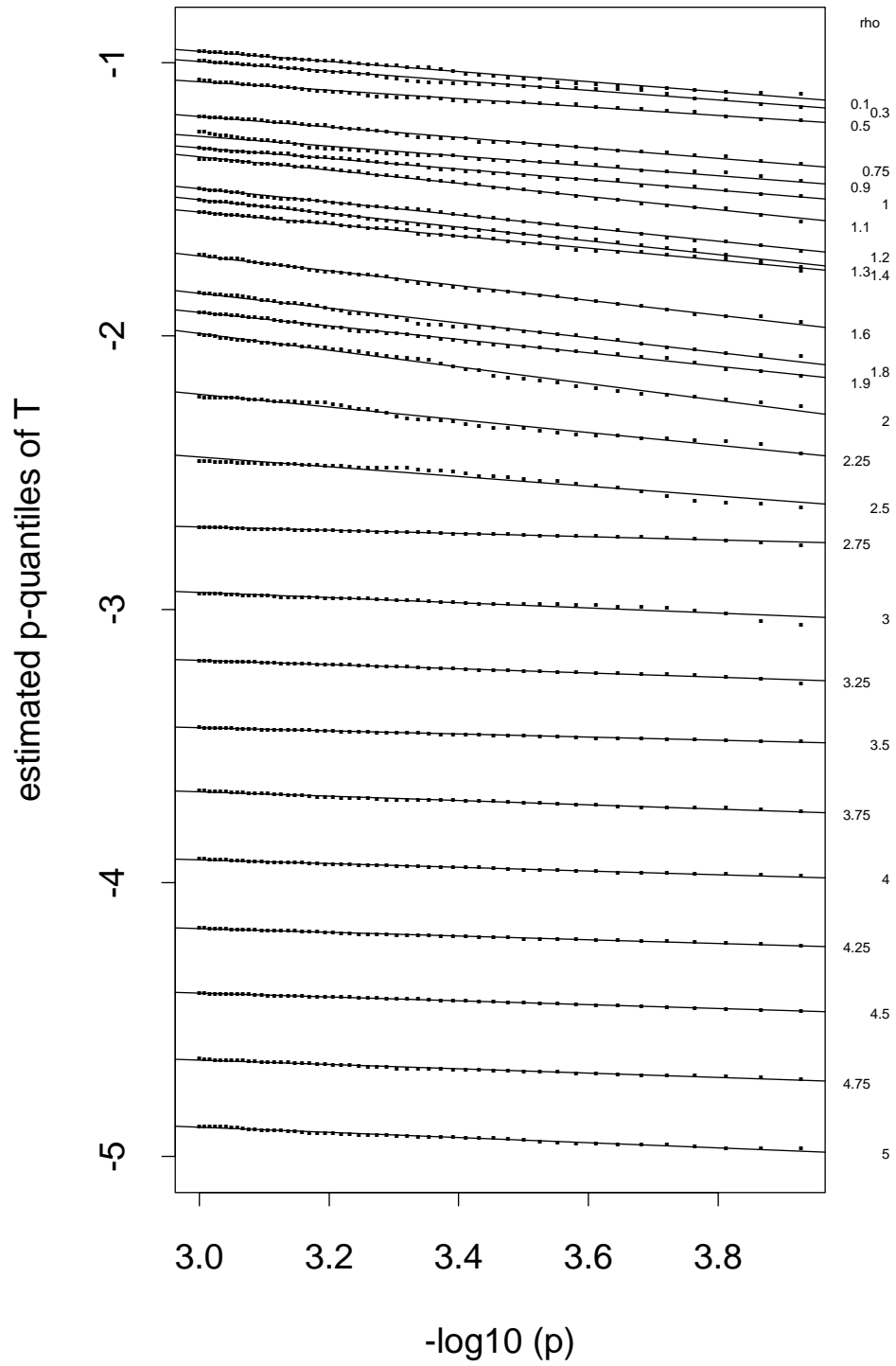


Figure 4. Estimated quantiles  $\hat{t}_p$ , for  $\kappa = 1$ ,  $\rho \in [.1, 5]$ , and 100,000 simulations

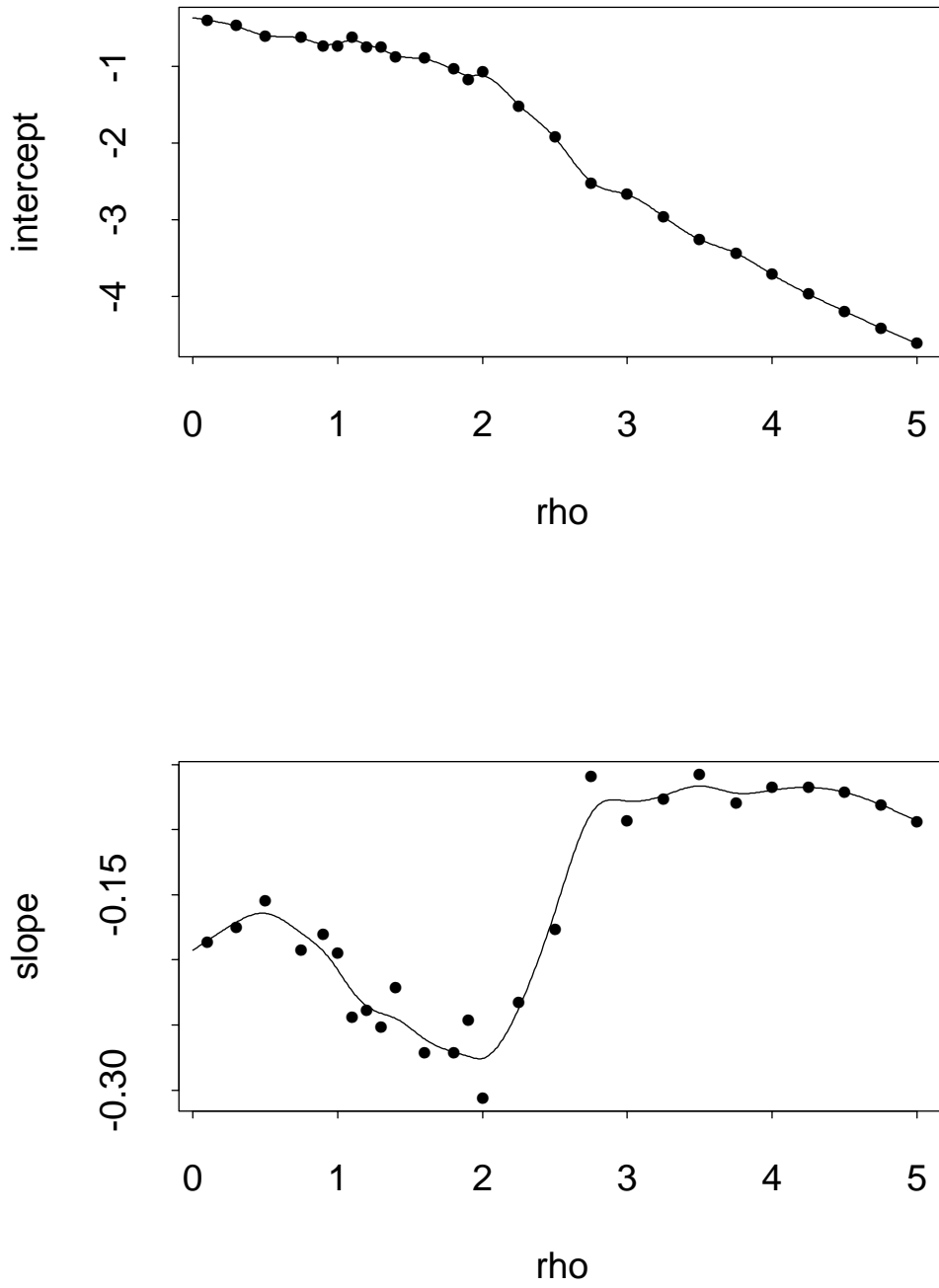


Figure 5. Estimated intercepts and slopes for linear relationship between  $-\log_{10}(p)$  and  $\hat{t}_p$  for  $\kappa = 1$

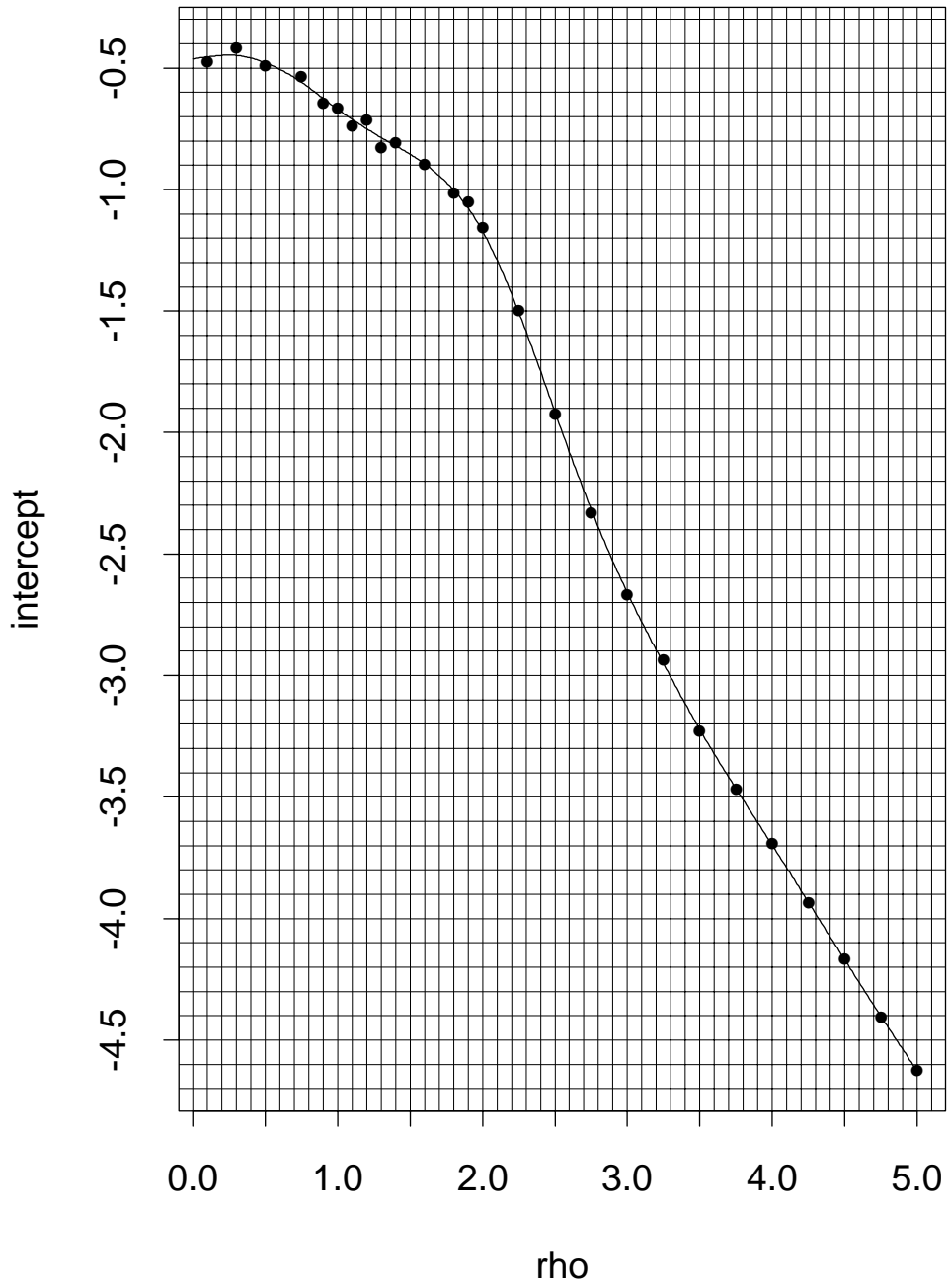


Figure 6. Average of 10 estimated intercepts for linear relationship between  $-\log_{10}(p)$  and  $\hat{t}_p$  for  $\kappa = 1$

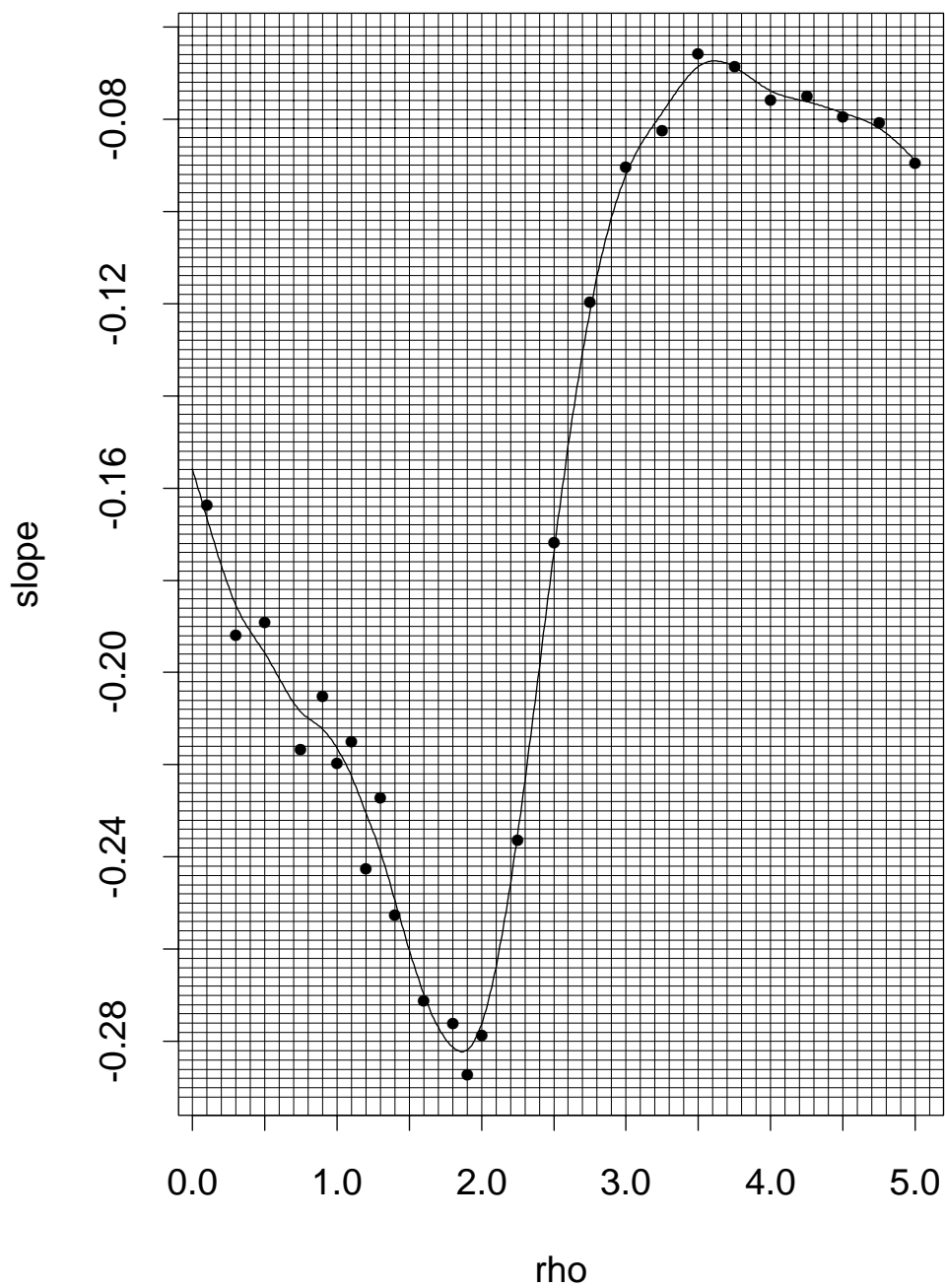


Figure 7. Average of 10 estimated slopes for linear relationship between  $-\log_{10}(p)$  and  $\hat{t}_p$  for  $\kappa = 1$



Table 1. Coefficients for linear relationship  
between  $-\log_{10}(p)$  and  $\hat{t}_p$

$\rho$	intercepts $\alpha(\rho)$					slopes $\beta(\rho)$				
	$\kappa$ 1/10	1/3	1/2	2/3	1	1/10	1/3	1/2	2/3	1
0.1	-0.432	-0.439	-0.424	-0.470	-0.455	-0.179	-0.171	-0.178	-0.162	-0.167
0.2	-0.425	-0.449	-0.437	-0.467	-0.448	-0.182	-0.174	-0.178	-0.169	-0.177
0.3	-0.421	-0.458	-0.450	-0.465	-0.448	-0.184	-0.176	-0.179	-0.175	-0.185
0.4	-0.425	-0.468	-0.462	-0.466	-0.459	-0.186	-0.179	-0.182	-0.182	-0.191
0.5	-0.438	-0.477	-0.474	-0.470	-0.479	-0.188	-0.183	-0.186	-0.188	-0.196
0.6	-0.460	-0.489	-0.487	-0.481	-0.505	-0.190	-0.186	-0.190	-0.194	-0.201
0.7	-0.488	-0.502	-0.503	-0.497	-0.539	-0.191	-0.190	-0.195	-0.200	-0.207
0.8	-0.516	-0.518	-0.521	-0.519	-0.580	-0.193	-0.194	-0.200	-0.205	-0.210
0.9	-0.541	-0.538	-0.542	-0.547	-0.625	-0.195	-0.198	-0.205	-0.210	-0.212
1.0	-0.563	-0.563	-0.566	-0.583	-0.670	-0.197	-0.202	-0.210	-0.215	-0.216
1.1	-0.585	-0.592	-0.593	-0.622	-0.712	-0.199	-0.206	-0.215	-0.219	-0.222
1.2	-0.607	-0.617	-0.621	-0.660	-0.750	-0.201	-0.210	-0.221	-0.224	-0.230
1.3	-0.635	-0.639	-0.654	-0.695	-0.786	-0.203	-0.214	-0.224	-0.230	-0.239
1.4	-0.666	-0.661	-0.689	-0.729	-0.820	-0.205	-0.218	-0.227	-0.236	-0.249
1.5	-0.699	-0.689	-0.727	-0.760	-0.855	-0.207	-0.222	-0.230	-0.243	-0.260
1.6	-0.734	-0.723	-0.765	-0.790	-0.895	-0.210	-0.225	-0.233	-0.250	-0.270
1.7	-0.768	-0.762	-0.802	-0.820	-0.942	-0.212	-0.227	-0.237	-0.256	-0.277
1.8	-0.801	-0.803	-0.840	-0.855	-1.001	-0.214	-0.229	-0.241	-0.262	-0.281
1.9	-0.832	-0.844	-0.878	-0.899	-1.076	-0.216	-0.232	-0.245	-0.267	-0.282
2.0	-0.861	-0.882	-0.914	-0.950	-1.172	-0.219	-0.234	-0.250	-0.270	-0.276
2.1	-0.893	-0.920	-0.951	-1.001	-1.291	-0.221	-0.237	-0.255	-0.271	-0.264
2.2	-0.926	-0.959	-0.988	-1.055	-1.429	-0.224	-0.241	-0.260	-0.271	-0.246
2.3	-0.959	-0.999	-1.027	-1.118	-1.583	-0.226	-0.245	-0.264	-0.268	-0.224
2.4	-0.991	-1.038	-1.067	-1.193	-1.748	-0.229	-0.249	-0.269	-0.262	-0.199
2.5	-1.025	-1.072	-1.109	-1.283	-1.915	-0.231	-0.254	-0.273	-0.254	-0.174
2.6	-1.061	-1.099	-1.156	-1.390	-2.081	-0.233	-0.260	-0.276	-0.243	-0.151
2.7	-1.100	-1.123	-1.207	-1.510	-2.240	-0.235	-0.265	-0.278	-0.229	-0.131
2.8	-1.137	-1.152	-1.266	-1.640	-2.390	-0.238	-0.271	-0.279	-0.213	-0.114
2.9	-1.174	-1.187	-1.337	-1.775	-2.530	-0.240	-0.275	-0.277	-0.197	-0.101
3.0	-1.211	-1.226	-1.423	-1.912	-2.660	-0.242	-0.278	-0.269	-0.179	-0.092
3.1	-1.251	-1.268	-1.526	-2.049	-2.781	-0.244	-0.280	-0.255	-0.162	-0.086
3.2	-1.290	-1.313	-1.644	-2.185	-2.895	-0.246	-0.281	-0.237	-0.144	-0.081
3.3	-1.327	-1.365	-1.768	-2.318	-3.007	-0.248	-0.280	-0.217	-0.128	-0.076
3.4	-1.361	-1.423	-1.894	-2.448	-3.116	-0.250	-0.277	-0.199	-0.114	-0.072
3.5	-1.397	-1.489	-2.019	-2.572	-3.222	-0.252	-0.272	-0.181	-0.101	-0.069
3.6	-1.435	-1.563	-2.142	-2.688	-3.323	-0.254	-0.266	-0.165	-0.090	-0.067
3.7	-1.476	-1.645	-2.262	-2.795	-3.419	-0.255	-0.257	-0.151	-0.081	-0.068
3.8	-1.519	-1.737	-2.380	-2.894	-3.513	-0.257	-0.247	-0.137	-0.075	-0.070
3.9	-1.562	-1.838	-2.496	-2.985	-3.605	-0.258	-0.235	-0.123	-0.070	-0.072
4.0	-1.605	-1.947	-2.608	-3.070	-3.698	-0.259	-0.222	-0.110	-0.067	-0.074
4.1	-1.648	-2.061	-2.716	-3.152	-3.792	-0.261	-0.209	-0.099	-0.066	-0.075
4.2	-1.689	-2.176	-2.820	-3.231	-3.886	-0.262	-0.194	-0.090	-0.066	-0.076
4.3	-1.725	-2.287	-2.919	-3.309	-3.981	-0.263	-0.180	-0.081	-0.066	-0.077
4.4	-1.758	-2.391	-3.013	-3.385	-4.076	-0.265	-0.167	-0.075	-0.067	-0.078
4.5	-1.793	-2.491	-3.102	-3.461	-4.170	-0.266	-0.154	-0.070	-0.069	-0.079
4.6	-1.834	-2.588	-3.184	-3.539	-4.263	-0.267	-0.142	-0.066	-0.070	-0.080
4.7	-1.880	-2.685	-3.262	-3.617	-4.356	-0.267	-0.130	-0.065	-0.072	-0.081
4.8	-1.931	-2.783	-3.334	-3.695	-4.448	-0.268	-0.118	-0.066	-0.073	-0.083
4.9	-1.984	-2.883	-3.402	-3.772	-4.538	-0.268	-0.107	-0.068	-0.075	-0.086
5.0	-2.038	-2.985	-3.468	-3.848	-4.627	-0.269	-0.095	-0.071	-0.077	-0.089

### 4.3 An Example Calculation

Here we illustrate the use of the above results in a specific although artificial example with  $\rho_1 = \rho_2$ . It is assumed the hole and pin diameters are toleranced respectively to the intervals  $[a, b] = [.098, .101]$  and  $[c, d] = [.09375, .09425]$  with nominal hole to pin clearance of

$$\eta = \frac{a + b}{2} - \frac{c + d}{2} = .0055 .$$

For the hole centering accuracy we assume that  $r = .01$ , i.e., 99.73% of all hole centers are located within radius  $r = .01$  of target. We also specify a risk of  $p = .001$  for no loose pinning of the two parts.

With these inputs we have  $\rho = \rho_1 = (b - a)/r = .003/.010 = .3$  and  $\rho_2 = (d - c)/r = .0005/.010 = .05$ , and thus  $\kappa = \rho_2/\rho_1 = 1/6$ . According to worst case considerations we have clearance

$$w_0 = a - d - 2r = .098 - .09425 - 2 \times .01 = -.01625 ,$$

i.e., we are .01625 away from any clearance at all.

For the statistical tolerance analysis we will use Table 1 for  $\kappa = 1/10$  and  $\kappa = 1/3$ , since  $\kappa = 1/6$  is not covered in Table 1. For  $\kappa = 1/10$  we read the following values from Table 1

$$\alpha(\rho) = \alpha(.3) = -.421 \quad \text{and} \quad \beta(\rho) = \beta(.3) = -.184$$

so that

$$\hat{t}_{.001}(.3) = \alpha(.3) + \beta(.3) [-\log_{10}(.001)] = -.973 .$$

For  $\kappa = 1/3$  we read the following values from Table 1

$$\alpha(\rho) = \alpha(.3) = -.458 \quad \text{and} \quad \beta(\rho) = \beta(.3) = -.176$$

so that

$$\hat{t}_{.001}(.3) = \alpha(.3) + \beta(.3) [-\log_{10}(.001)] = -.986 .$$

For  $\kappa = 1/6$  we take the interpolated value

$$\hat{t}_{.001}(.3) = -.973 + \frac{-.986 - (-.973)}{\frac{1}{3} - \frac{1}{10}} \left( \frac{1}{6} - \frac{1}{10} \right) = -.9767 .$$

Thus the statistically toleranced lower bound (with risk  $p = .001$ ) for the maximal minimum play  $P_{\max-\min}$  is

$$m_0 = \eta + r \hat{t}_{.001}(\rho) = .0055 - .01 \cdot .9767 = -.00427$$

which, although still negative, is considerably better than the worst case value  $w_0 = -.01625$ . Both calculations indicate either that the tolerances are not tight enough to assure the

assembly goal, since  $m_0$  and  $w_0$  are both negative, or that the nominal clearance  $\eta$  was chosen too small.

A larger  $\eta$  will lead to more slack after pinning of the parts and thus to freer motion and more misalignment of the parts relative to each other. From that perspective it is desirable to keep  $\eta$  small. However, if in relaxing  $\eta$  the misalignment consequences are still acceptable, one may go this route since it usually is most easily accommodated. It only involves a shift in the nominal clearance whereas all tolerance tightening would require a reduction in variability.

Taking the easier route of increasing the nominal clearance  $\eta$  we immediately see from the above calculations that the above nonclearance situation can be remedied by increasing  $\eta$  by .01625 to  $.0055 + .01625 = .02175$  in the worst case treatment and by .00427 to  $.0055 + .00427 = .00977$  in the statistical tolerance treatment. The worst case treatment thus requires 123% more nominal slack than is needed under statistical tolerancing. This extra slack is undesirable and unnecessary.

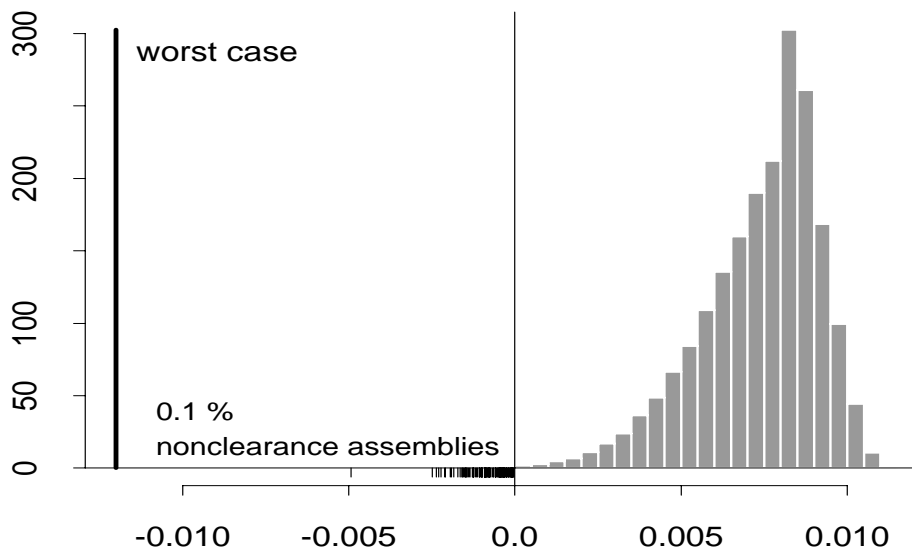


**Figure 8. Validation distribution of  $P_{\max-\min}$  after increasing the nominal clearance  $\eta$  by .00425 in 100,000 simulated assemblies**

Figure 8 shows a simulation of 100,000 assemblies after an increase of .00425 in the nominal tolerance  $\eta$ . The tickmarks below the axis show the 100 most extreme low clearance cases. All of them lie below zero which is consistent with the .11% nonassembly assessment. Recall, that we had aimed for .1% nonassembly.

Another way to deal with the shortfall in  $m_0$  and  $w_0$  is to tighten the tolerances. As pointed out above this is usually more difficult. Furthermore, the analysis of what tolerance

reduction may be required is not as simple as finding the required increase in  $\eta$ . The reason is that whereas  $\eta$  only appeared at the end of the calculations, after having dealt with looking up values from Table 1, the tolerances as represented by  $\rho_1$ ,  $\rho_2$  and  $r$  enter upfront. Thus one will have to proceed on a trial and error basis. We illustrate this here by finding out how much smaller  $r$  would need to be to make  $m_0$  and  $w_0$  positive.

Under worst case tolerancing to get  $w_0 > 0$  we need

$$0 < a - d - 2r = .00375 - 2r \quad \text{or} \quad r < .001875.$$

This is quite stringent, since it leads to a value that is over 5 times smaller than originally considered.

To see for which  $r$  we have  $m_0 > 0$  we proceed by trial and error. Let us try  $r = .005$ . Then  $\rho = \rho_1 = .003/.005 = .6$ ,  $\rho_2 = .0005/.005 = .1$ , and thus  $\kappa = \rho_2/\rho_1 = 1/6$  which again leads to interpolation between  $\kappa = 1/10$  and  $\kappa = 1/3$ . From Table 1 we get for  $\kappa = 1/10$  and  $\rho = .6$

$$\alpha(\rho) = \alpha(.6) = -.460 \quad \text{and} \quad \beta(\rho) = -.190$$

so that

$$\hat{t}_{.001}(\rho) = \alpha(\rho) + \beta(\rho) [-\log_{10}(.001)] = -1.03$$

and for  $\kappa = 1/3$  and  $\rho = .6$  we get from Table 1

$$\alpha(\rho) = \alpha(.6) = -.489 \quad \text{and} \quad \beta(\rho) = -.186$$

with

$$\hat{t}_{.001}(\rho) = \alpha(\rho) + \beta(\rho) [-\log_{10}(.001)] = -1.047.$$

Interpolating between these two values for  $\hat{t}_{.001}(\rho)$  we get the one for  $\kappa = 1/6$ , namely

$$\hat{t}_{.001}(.6) = -1.03 + \frac{-1.047 - (-1.03)}{\frac{1}{3} - \frac{1}{10}} \left( \frac{1}{6} - \frac{1}{10} \right) = -1.0349.$$

This results in

$$m_0 = \eta + r \hat{t}_{.001}(\rho) = .0055 - .005 \cdot 1.0349 = .000326; .$$

This is a positive clearance and relaxing the positioning tolerance to  $r = .0053$  we find by the same process  $m_0 = .000064$  and we will stop here.

Figure 9 shows the clearances  $P_{\max-\min}$  for 100,000 simulated assemblies after tightening the positioning tolerance to  $r = .0053$ . The hundred lowest clearances are indicated by the hanging tickmarks. Not all of these fall below zero, which is consistent with the positive value  $m_0 = .000064$ .

From the two validations represented in Figures 8 and 9 it appears that the interpolation exercise of using Table 1 in the above manner does preserve the targeted risk of .1% nonassemblies quite well.

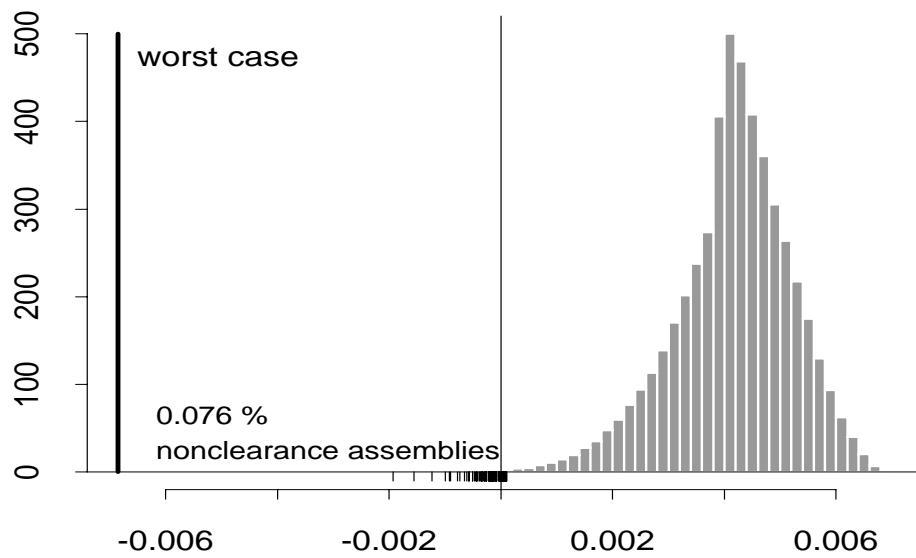
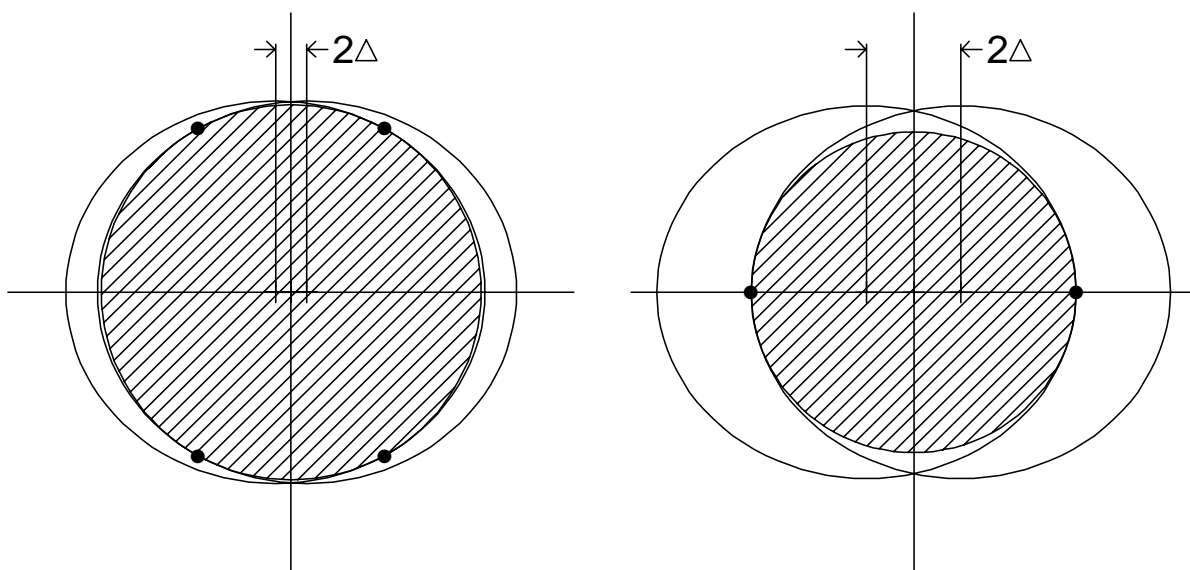


Figure 9. Validation distribution of  $P_{\max-\min}$  after tightening the position tolerance to  $r = .0053$  in 100,000 simulated assemblies

## 5 Variations in Perpendicularity

A further complication to the hole pinning problem arises when the parts to be pinned have significant thickness,  $W$ , and the holes are not necessarily drilled exactly perpendicular to the parallel part surfaces. In that case the entry and exit contour of the drilled hole are ellipses of identical shape but offset from each other along their common main axis. See Figure 10 for two typical projected views of these two ellipses. The shaded circle inscribed into the intersection of the ellipses represents the cross section of the largest cylindrical pin that could pass through such a hole in perpendicular fashion. The diameter  $D'$  of this shaded circle will be called the effective hole diameter. The two projected views differ in the number of contact points that the circle has with the ellipses.



**Figure 10. Maximal circle inscribed to two ellipses offset along main axis**

Focussing on the maximal diameter for perpendicular pin insertion is a somewhat conservative choice. It certainly simplifies the mathematics of the problem by reducing it to the previously studied clearance criterion when perpendicularity of holes was assumed. The reason why this may be conservative is that one may get pins with larger diameters through two such paired and slanted holes. However, we believe that the increase in diameter is small since the slants in the two holes and their position relative to each other typically will not be optimally aligned. Furthermore, even if a larger pin could be inserted this way it would have

to be at a slant and this would create possibly undesired stresses in the fastening process. By focussing on perpendicular pin insertion we avoid all these problems.

### 5.1 The Effective Hole Diameter

There are two effects that result from such angular deviations in the drilled hole axes. The first is a reduction of the hole diameter  $D$  to the effective diameter  $D'$ . The second effect is a  $\Delta$  dislocation of the inscribed effective hole center from the center of the entry ellipse. Here  $2\Delta \geq 0$  is the distance between the centers  $(0,0)$  and  $(X,Y)$  of the entry and exit contour ellipses of the hole when one ellipse is perpendicularly projected onto the plane of the other, see Figure 10. The quantity  $2\Delta$  expresses to what extent the hole deviates from perpendicularity ( $\Delta = 0$ ).

In Appendix B it is shown that the effective hole diameter is

$$\begin{aligned} D' &= D\sqrt{1 + \frac{4\Delta^2}{W^2}} - 2\Delta && \text{for } \frac{4\Delta^2}{W^2} \left( \frac{D^2}{W^2} - 1 \right) \leq 1 \\ &= \sqrt{D^2 - W^2} && \text{for } \frac{4\Delta^2}{W^2} \left( \frac{D^2}{W^2} - 1 \right) > 1. \end{aligned} \quad (4)$$

Here  $D$  is the diameter of the hole through the part as measured perpendicularly to the hole axis. It will be argued below that the second form of  $D'$ , namely  $\sqrt{D^2 - W^2}$ , is of little practical interest.

### 5.2 Modeling Nonperpendicularity Variations

It remains to formulate a reasonable model for the variations in  $2\Delta$ . Presumably the angular deviation  $\alpha$  from perpendicularity is usually very small, i.e.,  $2\Delta/W = \arctan(\alpha)$  is small. Since there appears to be no preference toward any direction in which the deviations from perpendicularity may take place, it seems reasonable to assume that  $(X,Y)$  have a circular symmetric distribution around the origin  $(0,0)$ . If we establish perpendicularity of the hole drilling tool independently along the  $X$  and  $Y$  directions and thus incur errors independently in those two directions we are again led to the circular symmetric, bivariate normal distribution around  $(0,0)$  as a reasonable model. The common standard deviation  $\tau = \tau_X = \tau_Y$  would usually be very small. Assuming that we deal with variation in the angle  $\alpha$  as the basic phenomenon it would be reasonable to assume that the standard deviation  $\tau$  governing the  $X, Y$  deflections is proportional to the part thickness  $W$ , i.e.,  $\tau = W\tau_1$ , where  $\tau_1$  corresponds to  $W = 1$ . With this notation the entry to exit hole center deflection  $2\Delta$  for a part with thickness  $W$  can be written

$$2\Delta = \sqrt{X^2 + Y^2}$$

and we have that

$$P(2\Delta \leq R) = 1 - \exp\left(-\frac{R^2}{2\tau^2}\right) = 1 - \exp\left(-\frac{R^2}{2W^2\tau_1^2}\right). \quad (5)$$

For small angles  $\alpha$  (in radians) or  $\alpha^\circ$  (in degrees), e.g., with  $|\alpha| \leq .052$  or  $|\alpha^\circ| \leq 3^\circ$ , the approximation

$$\frac{2\Delta}{W} = \arctan \alpha \approx \alpha$$

is excellent. Thus

$$P(\alpha \leq R) \approx P\left(\frac{2\Delta}{W} \leq R\right) = 1 - \exp\left(-\frac{R^2}{2\tau_1^2}\right)$$

or

$$P(\alpha^\circ \leq t) = P\left(\alpha \leq \frac{2\pi t}{360}\right) = 1 - \exp\left(-\frac{1}{2} \left[\frac{2\pi t}{360\tau_1}\right]^2\right).$$

Tolerancing  $\alpha^\circ$  by  $\bar{\alpha}^\circ = \bar{\alpha}^\circ(\gamma)$  such that

$$\gamma = P[\alpha^\circ \leq \bar{\alpha}^\circ]$$

yields the following relationship between  $\bar{\alpha}^\circ$ ,  $\tau_1$ , and  $\gamma$

$$\bar{\alpha}^\circ = \frac{360}{2\pi} \tau_1 \sqrt{-2 \log_e(1 - \gamma)}$$

which for  $\gamma = .9973$  becomes  $\bar{\alpha}^\circ = 197.06 \tau_1$  or  $\tau_1 = .005075 \bar{\alpha}^\circ$ . For example, a limit of  $\bar{\alpha}^\circ = 3^\circ$  on the angular deflections leads to  $\tau_1 = 3/197.06 = .01522$  and thus

$$.9973 = P(\alpha^\circ \leq 3^\circ) = P\left(\frac{2\Delta}{W} \leq \frac{2\pi}{360} 3\right) = P\left(\sqrt{X^2 + Y^2} \leq .05236 W\right)$$

for a part of thickness  $W$ .

If we limit the angular deflections to a very liberal  $3^\circ$ , then  $2\Delta/W \leq .052$  and the condition for the second case in (4) imply

$$\frac{D}{W} > \sqrt{1 + \frac{W^2}{4\Delta^2}} \geq \sqrt{1 + 1/.052^2} = 19.3.$$

This will hardly occur in practical situations and therefore we rule out the second case of (4) from further considerations, i.e., we assume from now on that

$$D' = D \sqrt{1 + \frac{4\Delta^2}{W^2}} - 2\Delta.$$

Using the excellent approximation  $\sqrt{1 + x^2} \approx 1 + x^2/2$  for  $|x| \leq .052$  we further simplify  $D'$  to

$$\begin{aligned} D' &\approx D \left(1 + \frac{2\Delta^2}{W^2}\right) - \frac{2\Delta}{W} W \\ &= D + \frac{D\tau_1^2}{2} Q^2 - \tau_1 W Q \quad \text{with } Q = \frac{2\Delta}{\tau_1 W} \\ &\approx D - \tau_1 W Q = D - 2\Delta \end{aligned}$$



where in the last approximation we omit the usually negligible term  $D\tau_1^2Q^2/2$ , but erring on the conservative side (for loose pinning) by making  $D'$  smaller in the rare situations when the neglected term is of any significance. The random variable  $Q$  has distribution function

$$P(Q \leq x) = 1 - \exp(-x^2/2) \quad \text{for} \quad x \geq 0 \quad (6)$$

and we see that  $P(0 \leq Q \leq 4) = .9997$ . This supports the above negligibility of the term  $D\tau_1^2Q^2/2$ .

From the form  $D' = D - \tau_1WQ$  we see that the part width  $W$  has a significant influence on the distribution of  $D'$ . Previously, when dealing with perpendicular holes only, we assumed a common uniform distribution for the hole diameters  $D_1, \dots, D_4$ . In principle, it is possible that by design we deal with four different part thicknesses  $W_1, \dots, W_4$  at the four hole locations. This in turn would lead to four different hole diameter distributions for  $D'_1, \dots, D'_4$ . Such complexity should more properly be handled by a software simulation tool with appropriate flexibility. A software tool with sufficient flexibility could easily be built based on the material given here. However, in the interest of complexity reduction we will deal here only with one part thickness  $W$  for both parts and thus with only one distribution for the effective hole diameters  $D'_1, \dots, D'_4$ .

It seems reasonable to assume that the angular deflection from the perpendicular is established just once against each part and that the two holes on the same part suffer from the same amount of angular deflection. However, at this point we leave open the possibility that the direction of drilling and thus the direction of deflection may rotate because of part rotation within the part surface plane. In that case the perpendicularity deflection  $2\Delta$  and thus  $Q$  will be the same for both holes on the same part. However, we assume that the perpendicularity deflections  $2\Delta_1$  and  $2\Delta_2$  are independent from part to part. We also may reasonably assume that the angular deflection tolerances are the same for both parts. In view of the approximation  $D'_i \approx D_i - \tau_1WQ_i$ ,  $i = 1, 2, 3, 4$ , with  $Q_1 = Q_2$  and  $Q_3 = Q_4$  and the earlier assumption that  $D_1 = D_2$  and  $D_3 = D_4$ , we can now similarly conclude that  $D'_1 = D'_2$  and  $D'_3 = D'_4$ .

As an aside, it is conceivable that parts of type  $i$  ( $i = 1, 2$ ) are massproduced in a jig and that it is the angle of the jig relative to the drilling tool that determines the angular deviation of the hole axis from the perpendicular. In that case this angular deviation would always be the same and would not change from part to part. Such a deviation, although random, would then have to be treated as a one time random effect. Since its size is not known but only bounded by the angular tolerance  $\bar{\alpha}^\circ$  we should treat that effect in worst case fashion, i.e., bound the term  $\tau_1WQ$  in the effective diameter  $D' = D - \tau_1WQ$  by  $B_0$  and then reduce the nominal diameter  $D_0$  and thus the nominal clearance  $\eta$  by  $B_0$ , while proceeding with the tolerance analysis as though we ignore perpendicularity deviations. As bound  $B_0$  on  $\tau_1WQ$  we can take

$$B_0 = (2\pi/360)\bar{\alpha}^\circ W = \sqrt{-2 \log_e(1 - .9973)} \tau_1 W$$

so that

$$P(\tau_1WQ \leq B_0) = P\left(Q \leq \sqrt{-2 \log_e(1 - .9973)}\right) = .9973 .$$

In reducing the analysis this way we also assume that the direction of the angularity deviation is the same for both holes on the same part. See the discussion below.

The second effect of nonperpendicularity is the effective hole center dislocation by the amount  $\Delta$ . This dislocation measures the distance of the effective hole center from the center of the hole entry ellipse. As such it compounds with the hole centering distribution which we view here as applying to the center of the hole entry ellipse. This compounding is best understood as adding to the center  $(U_i, V_i)$  of the hole entry ellipse the nonperpendicularity deflection vector  $(X_i/2, Y_i/2)$ , where

$$\Delta = \sqrt{(X_i/2)^2 + (Y_i/2)^2} = \frac{1}{2} \sqrt{X_i^2 + Y_i^2}.$$

Much of the following discussion will be dispensed with later, by assuming identical hole axis vectors for the two holes on the same part, and is given here only for possible use in a more flexible software simulation tool.

Previously we had modeled  $X_i$  and  $Y_i$  as independent normal random variables with common mean zero and standard deviation  $\tau = \tau_1 W$ , i.e.,  $(X_i, Y_i)$  has a bivariate normal distribution with mean vector  $(0, 0)$  and covariance matrix  $\tau^2 I_2$ , where  $I_2$  is a  $2 \times 2$  identity matrix. This is also expressed in the following symbolic notation

$$\begin{pmatrix} X_i \\ Y_i \end{pmatrix} \sim \mathcal{N}_2 \left( \begin{bmatrix} 0 \\ 0 \end{bmatrix}, \tau^2 I_2 \right).$$

We can reasonably assume that  $(U_i, V_i)$  and  $(X_i/2, Y_i/2)$  are independent of each other so that

$$\begin{pmatrix} U_i \\ V_i \end{pmatrix} \sim \mathcal{N}_2 \left( \begin{bmatrix} \mu_i \\ \nu_i \end{bmatrix}, \sigma^2 I_2 \right) \quad \text{and} \quad \begin{pmatrix} X_i/2 \\ Y_i/2 \end{pmatrix} \sim \mathcal{N}_2 \left( \begin{bmatrix} 0 \\ 0 \end{bmatrix}, (\tau/2)^2 I_2 \right)$$

$$\implies \begin{pmatrix} U'_i \\ V'_i \end{pmatrix} = \begin{pmatrix} U_i + X_i/2 \\ V_i + Y_i/2 \end{pmatrix} \sim \mathcal{N}_2 \left( \begin{bmatrix} \mu_i \\ \nu_i \end{bmatrix}, (\sigma^2 + \tau^2/4) I_2 \right) = \mathcal{N}_2 \left( \begin{bmatrix} \mu_i \\ \nu_i \end{bmatrix}, \sigma'^2 I_2 \right)$$

with  $\sigma'^2 = \sigma^2 + \tau^2/4 = \sigma^2 + W^2 \tau_1^2/4$ .

We denote by  $X'_i$  the distance between the effective hole centers on part  $i$ . Of interest is again the difference  $X'_1 - X'_2$ . This corresponds to the difference  $X_1 - X_2$  when perpendicularity was assumed as given. There it was shown that  $X_1 - X_2 \sim \mathcal{N}(0, 4\sigma^2)$ . The question is whether we can similarly assume that  $X'_1 - X'_2 \sim \mathcal{N}(0, 4\sigma'^2)$ . This depends on the nature of the perpendicularity errors on the same part. If the perpendicularity error vectors are the same for the two holes on the same part, i.e., the part was not rotated within the part plane between drilling operations, then the distance  $X'_i$  is the same as the distance  $X_i$ , i.e., the perpendicularity errors do not affect the effective hole center distances. In that case we have  $X'_1 - X'_2 = X_1 - X_2 \sim \mathcal{N}(0, 4\sigma^2)$ . Furthermore, in this case  $X'_1 - X'_2$ ,  $D'_1$ ,  $D'_3$ ,  $d_1$ , and  $d_2$  are all independent. This simplifies matters greatly when trying to study the distribution of

the resulting reduced clearance criterion  $P'_{\max-\min}$ , obtained from the expression for  $P_{\max-\min}$  with  $D_i$  replaced by  $D'_i$ , i.e.,

$$P'_{\max-\min} = \frac{D'_1 + D'_3}{2} - \frac{d_1 + d_2}{2} - \frac{1}{2} \max(|X_1 - X_2|, |D'_1 - D'_3| + |d_1 - d_2|) .$$

If however, the part was rotated within the part plane between drilling operations, we are faced with significant complications. Not only will this affect the distribution of  $X'_1 - X'_2$ , but it will also create some dependence between  $X'_1 - X'_2$  and the effective hole diameters  $D'_1$  and  $D'_3$ , since both are driven by the common random variables  $Q_1$  and  $Q_3$ . Furthermore, such a rotation may not be uniform over the interval  $[0, 2\pi]$  as would be implied by complete independence of perpendicularity errors from hole to hole. It would be implausible to have independent drill orientation errors when drilling holes into the same flat surface, since the orientation would presumably be established against that surface. Without information on the drilling process it may be quite difficult to establish reasonable distributional assumptions concerning such rotations. For that reason we will exclude rotations of the drilling axis while moving the drilling tool from one hole to the next on the same part. This may not be a great loss since usually the work piece is clamped down and it is the numerically controlled drill tool that moves along simple translations and not by rotations.

### 5.3 The Standardized Clearance Distribution

The distribution of any one effective hole diameter  $D'_i = D_i - \tau_1 W Q_i$  is no longer uniform but is derived from the uniform distribution of  $D_i$  and the distribution of  $Q_i$  given in (6). As before we normalize  $D'_i$  by considering

$$\frac{D'_i - D_0}{r} = \frac{D_i - D_0}{r} - \frac{\tau_1 W}{r} Q_i = \rho_1 V_i - \rho_3 Q_i = \rho_1 (V_i - \omega Q_i)$$

with  $\rho_3 = \tau_1 W/r$  and  $\omega = \rho_3/\rho_1$ . Again it would be complicated to derive the distribution of  $(D'_i - D_0)/r$  analytically and that would only be a stepping stone to the much more complicated distribution of  $P'_{\max-\min}$ . To get an appreciation of the distribution shapes for  $(D'_i - D_0)/r$  we again employ simulations. Since  $\rho_1$  acts as simple scale parameter in  $\rho_1 (V_i - \omega Q_i)$  it suffices to simulate the distributions of  $V_i - \omega Q_i$  for a selection of  $\omega$  values. The resulting histograms are given in Figure 11 and exhibit a variety of shapes, ranging from a near uniform distribution, dominated by  $V_i$ , to a distribution dominated by  $-\omega Q_i$ .

As before we will study the distribution of  $P'_{\max-\min}$  in its standardized form, namely  $(P'_{\max-\min} - \eta)/r$  which has the same distribution as

$$\begin{aligned} T' &= \frac{1}{2} (V_1 + V_3) \rho_1 - \frac{1}{2} (\tilde{V}_1 + \tilde{V}_2) \rho_2 - \frac{1}{2} (Q_1 + Q_3) \rho_3 \\ &\quad - \frac{1}{2} \max \left( .5815 |Z|, |\rho_1 (V_1 - V_3) - \rho_3 (Q_1 - Q_3)| + |\tilde{V}_1 - \tilde{V}_2| \rho_2 \right) \\ &= \rho_1 \frac{1}{2} \left[ V_1 + V_3 - \omega (Q_1 + Q_3) - \kappa (\tilde{V}_1 + \tilde{V}_2) \right] \\ &\quad - \frac{1}{2} \max \left( .5815 |Z|, \rho_1 \left[ |V_1 - V_3 - \omega (Q_1 - Q_3)| + \kappa |\tilde{V}_1 - \tilde{V}_2| \right] \right) \end{aligned}$$

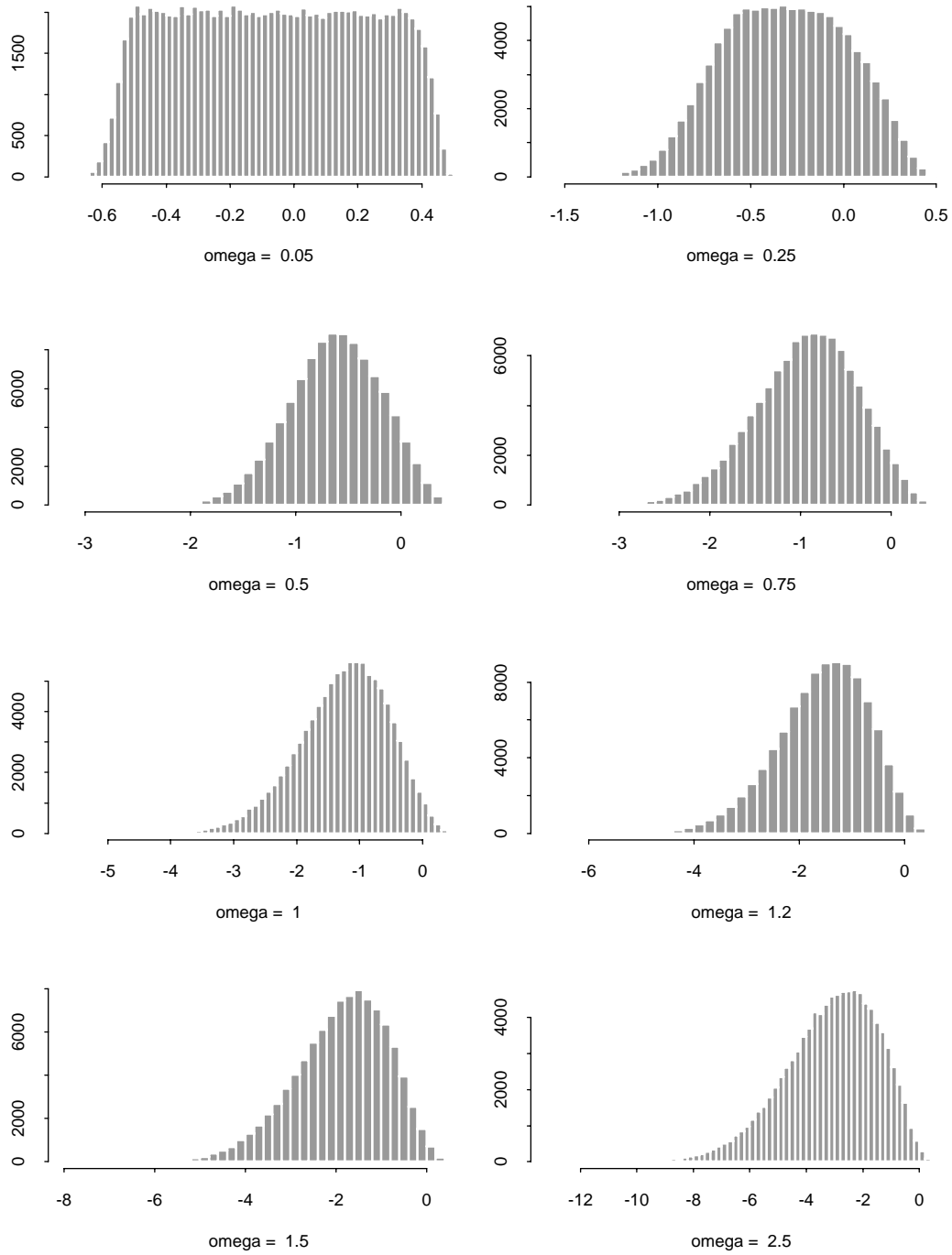


Figure 11. Simulated distributions of  $V_i - \omega Q_i$ , for various values of  $\omega$ , from 100,000 simulations

where  $V_1, V_3, \tilde{V}_1$  and  $\tilde{V}_2$  are uniformly distributed over  $[-\frac{1}{2}, \frac{1}{2}]$ , and  $Q_1$  and  $Q_2$  have distribution function (6). Furthermore, all six random variables are independent of each other. The distribution of  $T'$  can again be studied via simulations for various combinations of  $\rho = \rho_1$ ,  $\kappa = \rho_2/\rho_1$ , and  $\omega = \rho_3/\rho_1$ .

Adding the nonperpendicularity component into our tolerancing considerations unfortunately has added one new parameter, namely  $\rho_3$  or  $\omega$ , into the tolerance analysis for  $P'_{\max-\min}$ . To cover an appropriate range for  $\omega = \rho_3/\rho_1 = \tau_1 W/(b-a)$  we offer the following considerations. The numerator of  $\omega = \tau_1 W/(b-a)$  controls the deflection  $2\Delta$  of entry to exit hole centers, namely from (5) we have

$$P(2\Delta \leq k\tau_1 W) = 1 - \exp\left(-\frac{k^2}{2}\right) = .9973 \quad \text{for} \quad k = \sqrt{-2 \log_e(1 - .9973)} = 3.439 .$$

Since  $2\Delta$  is the amount by which  $D$  is reduced to  $D'$  It seems that this bound on  $2\Delta$  should be somewhat comparable to the tolerance range  $b-a$  on the hole diameter. Thus we propose to look at values

$$k\omega = \frac{k\tau_1 W}{b-a} = .5, 1, 1.5, 2 .$$

Using round numbers this translates roughly to

$$\omega = \frac{\tau_1 W}{b-a} = \frac{2\pi}{360 \sqrt{-2 \log_e(1 - .9973)}} \frac{W \bar{\alpha}^\circ}{b-a} = .005075 \frac{W \bar{\alpha}^\circ}{b-a} = .15, .30, .45, .60 ,$$

where  $\bar{\alpha}^\circ$  is the tolerance bound (in degrees) on the angular deviation from perpendicularity.

It now remains to carry out the same programme of simulations as before, leading to four new tables, Tables 2-5, corresponding to Table 1, one table for each  $\omega$ . These tables can be used in conjunction with Table 1, which corresponds to  $\omega = 0$ , to do the necessary interpolations. This is illustrated by example calculations in the next section.

#### 5.4 Worst Case Clearance under Nonperpendicularity

How does the nonperpendicularity tolerance affect worst case tolerancing? Previously, when perpendicularity was assumed the worst case clearance was

$$w_0 = a - d - 2r ,$$

where  $a$  was the lowest tolerated hole diameter value. From the assumptions and approximations made above we see that nonperpendicularity only affects the effective hole size in that  $D_i$  is replaced by  $D'_i = D_i - 2\Delta_i (\leq D_i)$ . A lower tolerance bound  $a$  on  $D_i$  combined with an upper tolerance bound  $k\tau_1 W = .01745 \bar{\alpha}^\circ W$  for  $2\Delta_i$  leads to a lower tolerance value  $a - .01745 \bar{\alpha}^\circ W$  for  $D'_i$  and thus a worst case clearance value of

$$w'_0 = a - .01745 \bar{\alpha}^\circ W - d - 2r .$$

**Table 2. Coefficients for linear relationship  
between  $-\log_{10}(p)$  and  $\hat{t}_p$  for  $\omega = .15$**

$\rho$	intercepts $\alpha(\rho)$					slopes $\beta(\rho)$				
	$\kappa$ 1/10	1/3	1/2	2/3	1	1/10	1/3	1/2	2/3	1
0.1	-0.448	-0.412	-0.415	-0.425	-0.457	-0.173	-0.184	-0.174	-0.178	-0.171
0.2	-0.478	-0.450	-0.447	-0.452	-0.490	-0.176	-0.185	-0.179	-0.184	-0.178
0.3	-0.508	-0.487	-0.479	-0.480	-0.523	-0.179	-0.185	-0.184	-0.190	-0.184
0.4	-0.540	-0.523	-0.512	-0.509	-0.558	-0.182	-0.187	-0.190	-0.195	-0.190
0.5	-0.572	-0.559	-0.547	-0.541	-0.592	-0.185	-0.189	-0.195	-0.201	-0.197
0.6	-0.606	-0.595	-0.585	-0.577	-0.625	-0.188	-0.192	-0.200	-0.206	-0.204
0.7	-0.642	-0.633	-0.625	-0.618	-0.662	-0.191	-0.195	-0.205	-0.211	-0.211
0.8	-0.679	-0.673	-0.670	-0.667	-0.707	-0.195	-0.199	-0.209	-0.214	-0.217
0.9	-0.718	-0.715	-0.720	-0.723	-0.765	-0.198	-0.203	-0.212	-0.217	-0.221
1.0	-0.757	-0.761	-0.775	-0.787	-0.839	-0.202	-0.206	-0.215	-0.219	-0.224
1.1	-0.799	-0.812	-0.835	-0.858	-0.929	-0.205	-0.210	-0.217	-0.219	-0.224
1.2	-0.843	-0.868	-0.901	-0.938	-1.036	-0.208	-0.212	-0.218	-0.219	-0.222
1.3	-0.892	-0.932	-0.973	-1.025	-1.161	-0.211	-0.213	-0.219	-0.217	-0.219
1.4	-0.946	-1.002	-1.051	-1.120	-1.294	-0.214	-0.213	-0.219	-0.216	-0.216
1.5	-1.006	-1.078	-1.133	-1.220	-1.426	-0.216	-0.213	-0.218	-0.214	-0.213
1.6	-1.071	-1.157	-1.219	-1.323	-1.554	-0.218	-0.213	-0.218	-0.212	-0.212
1.7	-1.140	-1.239	-1.308	-1.428	-1.679	-0.220	-0.213	-0.217	-0.212	-0.211
1.8	-1.212	-1.323	-1.399	-1.532	-1.799	-0.222	-0.214	-0.218	-0.213	-0.213
1.9	-1.286	-1.408	-1.492	-1.635	-1.912	-0.224	-0.216	-0.219	-0.216	-0.216
2.0	-1.360	-1.493	-1.584	-1.734	-2.021	-0.226	-0.218	-0.222	-0.220	-0.221
2.1	-1.435	-1.577	-1.676	-1.830	-2.127	-0.230	-0.222	-0.225	-0.226	-0.228
2.2	-1.509	-1.661	-1.767	-1.925	-2.234	-0.233	-0.226	-0.231	-0.233	-0.235
2.3	-1.583	-1.743	-1.858	-2.019	-2.345	-0.238	-0.232	-0.237	-0.240	-0.243
2.4	-1.657	-1.823	-1.947	-2.113	-2.458	-0.243	-0.239	-0.244	-0.247	-0.251
2.5	-1.730	-1.900	-2.034	-2.207	-2.570	-0.249	-0.247	-0.252	-0.255	-0.260
2.6	-1.802	-1.975	-2.120	-2.299	-2.675	-0.255	-0.256	-0.260	-0.264	-0.271
2.7	-1.873	-2.048	-2.205	-2.389	-2.772	-0.262	-0.267	-0.270	-0.273	-0.282
2.8	-1.943	-2.121	-2.288	-2.477	-2.861	-0.270	-0.277	-0.280	-0.283	-0.294
2.9	-2.013	-2.193	-2.369	-2.563	-2.946	-0.278	-0.287	-0.290	-0.294	-0.307
3.0	-2.082	-2.266	-2.448	-2.649	-3.035	-0.286	-0.298	-0.302	-0.305	-0.319
3.1	-2.151	-2.339	-2.526	-2.734	-3.133	-0.296	-0.308	-0.314	-0.316	-0.332
3.2	-2.218	-2.413	-2.603	-2.818	-3.236	-0.305	-0.319	-0.327	-0.327	-0.344
3.3	-2.284	-2.487	-2.681	-2.902	-3.336	-0.315	-0.329	-0.339	-0.339	-0.355
3.4	-2.349	-2.563	-2.758	-2.984	-3.431	-0.326	-0.339	-0.351	-0.351	-0.367
3.5	-2.413	-2.639	-2.836	-3.065	-3.524	-0.337	-0.348	-0.363	-0.363	-0.379
3.6	-2.474	-2.714	-2.914	-3.145	-3.619	-0.348	-0.358	-0.373	-0.376	-0.390
3.7	-2.535	-2.787	-2.994	-3.225	-3.719	-0.359	-0.368	-0.383	-0.389	-0.401
3.8	-2.595	-2.861	-3.075	-3.305	-3.828	-0.370	-0.378	-0.392	-0.402	-0.411
3.9	-2.655	-2.934	-3.157	-3.386	-3.943	-0.381	-0.388	-0.400	-0.414	-0.421
4.0	-2.717	-3.007	-3.240	-3.467	-4.053	-0.392	-0.398	-0.408	-0.427	-0.431
4.1	-2.781	-3.081	-3.322	-3.549	-4.152	-0.402	-0.408	-0.417	-0.439	-0.442
4.2	-2.846	-3.155	-3.404	-3.632	-4.242	-0.413	-0.418	-0.426	-0.450	-0.455
4.3	-2.913	-3.229	-3.486	-3.716	-4.331	-0.423	-0.429	-0.436	-0.461	-0.467
4.4	-2.981	-3.302	-3.566	-3.802	-4.423	-0.433	-0.439	-0.446	-0.472	-0.480
4.5	-3.051	-3.377	-3.646	-3.887	-4.518	-0.442	-0.450	-0.457	-0.483	-0.492
4.6	-3.122	-3.453	-3.725	-3.971	-4.619	-0.452	-0.460	-0.469	-0.494	-0.504
4.7	-3.194	-3.530	-3.804	-4.054	-4.721	-0.461	-0.469	-0.481	-0.505	-0.516
4.8	-3.265	-3.607	-3.882	-4.138	-4.822	-0.470	-0.479	-0.493	-0.516	-0.528
4.9	-3.336	-3.684	-3.959	-4.224	-4.918	-0.480	-0.488	-0.506	-0.526	-0.540
5.0	-3.407	-3.761	-4.037	-4.311	-5.013	-0.489	-0.498	-0.518	-0.536	-0.552

**Table 3. Coefficients for linear relationship  
between  $-\log_{10}(p)$  and  $\hat{t}_p$  for  $\omega = .30$**

$\rho$	intercepts $\alpha(\rho)$					slopes $\beta(\rho)$				
	$\kappa$ 1/10	1/3	1/2	2/3	1	1/10	1/3	1/2	2/3	1
0.1	-0.453	-0.446	-0.425	-0.459	-0.442	-0.171	-0.164	-0.172	-0.168	-0.173
0.2	-0.505	-0.504	-0.489	-0.516	-0.505	-0.175	-0.169	-0.176	-0.172	-0.178
0.3	-0.557	-0.562	-0.552	-0.575	-0.568	-0.179	-0.174	-0.181	-0.176	-0.184
0.4	-0.610	-0.622	-0.618	-0.636	-0.634	-0.184	-0.180	-0.186	-0.180	-0.189
0.5	-0.664	-0.683	-0.685	-0.701	-0.705	-0.188	-0.186	-0.190	-0.185	-0.195
0.6	-0.722	-0.747	-0.756	-0.770	-0.784	-0.193	-0.192	-0.195	-0.190	-0.201
0.7	-0.783	-0.814	-0.831	-0.846	-0.872	-0.199	-0.198	-0.199	-0.195	-0.207
0.8	-0.849	-0.886	-0.910	-0.929	-0.971	-0.205	-0.205	-0.204	-0.202	-0.213
0.9	-0.920	-0.962	-0.993	-1.020	-1.081	-0.211	-0.212	-0.210	-0.209	-0.219
1.0	-0.998	-1.043	-1.081	-1.119	-1.198	-0.219	-0.221	-0.216	-0.217	-0.226
1.1	-1.082	-1.127	-1.172	-1.223	-1.320	-0.227	-0.231	-0.225	-0.226	-0.235
1.2	-1.170	-1.214	-1.266	-1.330	-1.443	-0.237	-0.242	-0.236	-0.238	-0.247
1.3	-1.262	-1.303	-1.362	-1.437	-1.567	-0.247	-0.254	-0.250	-0.252	-0.261
1.4	-1.356	-1.395	-1.460	-1.543	-1.691	-0.259	-0.268	-0.265	-0.267	-0.277
1.5	-1.450	-1.488	-1.559	-1.649	-1.814	-0.273	-0.283	-0.282	-0.284	-0.295
1.6	-1.544	-1.582	-1.660	-1.753	-1.937	-0.287	-0.299	-0.300	-0.303	-0.313
1.7	-1.637	-1.678	-1.762	-1.856	-2.059	-0.303	-0.317	-0.319	-0.322	-0.332
1.8	-1.729	-1.774	-1.864	-1.959	-2.180	-0.320	-0.334	-0.338	-0.342	-0.352
1.9	-1.820	-1.871	-1.966	-2.065	-2.300	-0.338	-0.353	-0.357	-0.363	-0.372
2.0	-1.909	-1.968	-2.069	-2.174	-2.420	-0.356	-0.371	-0.377	-0.382	-0.393
2.1	-1.996	-2.064	-2.172	-2.285	-2.540	-0.375	-0.390	-0.396	-0.402	-0.412
2.2	-2.081	-2.162	-2.275	-2.399	-2.661	-0.395	-0.409	-0.415	-0.421	-0.432
2.3	-2.164	-2.260	-2.378	-2.514	-2.781	-0.415	-0.428	-0.434	-0.440	-0.453
2.4	-2.247	-2.359	-2.482	-2.628	-2.900	-0.436	-0.447	-0.452	-0.459	-0.473
2.5	-2.330	-2.460	-2.586	-2.739	-3.020	-0.456	-0.465	-0.471	-0.478	-0.493
2.6	-2.417	-2.561	-2.691	-2.845	-3.141	-0.476	-0.484	-0.490	-0.498	-0.513
2.7	-2.505	-2.664	-2.795	-2.947	-3.263	-0.496	-0.501	-0.509	-0.519	-0.532
2.8	-2.596	-2.767	-2.900	-3.045	-3.388	-0.515	-0.519	-0.528	-0.541	-0.551
2.9	-2.688	-2.870	-3.006	-3.141	-3.514	-0.535	-0.537	-0.548	-0.563	-0.569
3.0	-2.782	-2.973	-3.112	-3.238	-3.643	-0.554	-0.554	-0.567	-0.585	-0.586
3.1	-2.878	-3.075	-3.218	-3.339	-3.773	-0.572	-0.573	-0.587	-0.606	-0.602
3.2	-2.974	-3.176	-3.326	-3.445	-3.904	-0.591	-0.591	-0.606	-0.625	-0.619
3.3	-3.070	-3.277	-3.434	-3.556	-4.033	-0.609	-0.610	-0.625	-0.644	-0.636
3.4	-3.164	-3.377	-3.543	-3.671	-4.161	-0.628	-0.629	-0.643	-0.662	-0.653
3.5	-3.255	-3.476	-3.654	-3.788	-4.286	-0.646	-0.648	-0.660	-0.679	-0.671
3.6	-3.342	-3.573	-3.767	-3.902	-4.407	-0.665	-0.667	-0.674	-0.697	-0.690
3.7	-3.428	-3.670	-3.880	-4.016	-4.525	-0.684	-0.687	-0.688	-0.715	-0.710
3.8	-3.515	-3.765	-3.993	-4.130	-4.641	-0.702	-0.707	-0.701	-0.733	-0.730
3.9	-3.606	-3.858	-4.103	-4.244	-4.757	-0.720	-0.727	-0.714	-0.751	-0.751
4.0	-3.703	-3.951	-4.212	-4.357	-4.875	-0.737	-0.748	-0.729	-0.770	-0.771
4.1	-3.805	-4.043	-4.317	-4.469	-4.999	-0.753	-0.769	-0.744	-0.789	-0.789
4.2	-3.912	-4.135	-4.419	-4.579	-5.126	-0.769	-0.790	-0.762	-0.809	-0.807
4.3	-4.021	-4.228	-4.515	-4.689	-5.254	-0.784	-0.810	-0.783	-0.830	-0.824
4.4	-4.130	-4.322	-4.606	-4.795	-5.381	-0.799	-0.831	-0.807	-0.851	-0.842
4.5	-4.239	-4.417	-4.693	-4.895	-5.503	-0.814	-0.851	-0.833	-0.874	-0.862
4.6	-4.346	-4.514	-4.778	-4.987	-5.618	-0.828	-0.870	-0.860	-0.898	-0.884
4.7	-4.452	-4.610	-4.861	-5.069	-5.725	-0.843	-0.890	-0.887	-0.924	-0.910
4.8	-4.556	-4.704	-4.942	-5.142	-5.823	-0.858	-0.911	-0.916	-0.952	-0.938
4.9	-4.660	-4.797	-5.021	-5.210	-5.913	-0.874	-0.932	-0.944	-0.980	-0.969
5.0	-4.763	-4.888	-5.100	-5.274	-5.999	-0.889	-0.953	-0.974	-1.009	-1.001

Table 4. Coefficients for linear relationship  
between  $-\log_{10}(p)$  and  $\hat{t}_p$  for  $\omega = .45$

$\rho$	intercepts $\alpha(\rho)$					slopes $\beta(\rho)$				
	$\kappa$ 1/10	1/3	1/2	2/3	1	1/10	1/3	1/2	2/3	1
0.1	-0.446	-0.445	-0.441	-0.433	-0.450	-0.157	-0.155	-0.167	-0.169	-0.167
0.2	-0.535	-0.536	-0.535	-0.528	-0.541	-0.166	-0.165	-0.173	-0.175	-0.176
0.3	-0.623	-0.628	-0.629	-0.624	-0.635	-0.175	-0.174	-0.179	-0.181	-0.184
0.4	-0.713	-0.722	-0.725	-0.724	-0.733	-0.185	-0.184	-0.186	-0.188	-0.194
0.5	-0.804	-0.818	-0.822	-0.828	-0.837	-0.195	-0.195	-0.194	-0.196	-0.205
0.6	-0.897	-0.918	-0.923	-0.937	-0.950	-0.207	-0.206	-0.204	-0.206	-0.216
0.7	-0.992	-1.021	-1.025	-1.049	-1.071	-0.220	-0.219	-0.216	-0.218	-0.230
0.8	-1.091	-1.128	-1.131	-1.166	-1.199	-0.234	-0.233	-0.231	-0.233	-0.245
0.9	-1.193	-1.239	-1.239	-1.284	-1.333	-0.251	-0.249	-0.250	-0.252	-0.264
1.0	-1.297	-1.353	-1.349	-1.402	-1.470	-0.270	-0.266	-0.273	-0.274	-0.286
1.1	-1.404	-1.469	-1.462	-1.519	-1.610	-0.291	-0.286	-0.299	-0.299	-0.310
1.2	-1.512	-1.587	-1.578	-1.637	-1.753	-0.314	-0.308	-0.327	-0.327	-0.336
1.3	-1.623	-1.705	-1.698	-1.753	-1.897	-0.338	-0.332	-0.355	-0.357	-0.363
1.4	-1.737	-1.824	-1.821	-1.870	-2.044	-0.363	-0.358	-0.383	-0.388	-0.390
1.5	-1.852	-1.942	-1.946	-1.991	-2.190	-0.389	-0.385	-0.411	-0.419	-0.418
1.6	-1.968	-2.061	-2.073	-2.116	-2.337	-0.416	-0.414	-0.439	-0.450	-0.447
1.7	-2.085	-2.180	-2.203	-2.247	-2.484	-0.444	-0.443	-0.465	-0.480	-0.475
1.8	-2.203	-2.300	-2.333	-2.383	-2.630	-0.472	-0.472	-0.491	-0.509	-0.504
1.9	-2.321	-2.422	-2.463	-2.521	-2.775	-0.500	-0.502	-0.518	-0.537	-0.533
2.0	-2.440	-2.545	-2.592	-2.659	-2.919	-0.527	-0.530	-0.547	-0.566	-0.562
2.1	-2.560	-2.671	-2.719	-2.794	-3.061	-0.555	-0.558	-0.577	-0.594	-0.592
2.2	-2.682	-2.797	-2.846	-2.927	-3.201	-0.582	-0.586	-0.608	-0.622	-0.622
2.3	-2.804	-2.923	-2.974	-3.062	-3.338	-0.608	-0.614	-0.638	-0.649	-0.652
2.4	-2.928	-3.049	-3.102	-3.198	-3.475	-0.634	-0.642	-0.668	-0.676	-0.683
2.5	-3.053	-3.174	-3.232	-3.336	-3.614	-0.660	-0.670	-0.697	-0.702	-0.713
2.6	-3.180	-3.297	-3.362	-3.477	-3.760	-0.686	-0.698	-0.725	-0.727	-0.741
2.7	-3.306	-3.420	-3.493	-3.619	-3.912	-0.711	-0.726	-0.753	-0.752	-0.767
2.8	-3.431	-3.542	-3.626	-3.764	-4.069	-0.738	-0.754	-0.780	-0.776	-0.791
2.9	-3.552	-3.663	-3.761	-3.910	-4.231	-0.765	-0.783	-0.805	-0.800	-0.815
3.0	-3.670	-3.784	-3.897	-4.055	-4.395	-0.793	-0.812	-0.829	-0.824	-0.837
3.1	-3.785	-3.903	-4.032	-4.199	-4.561	-0.823	-0.841	-0.852	-0.849	-0.859
3.2	-3.896	-4.021	-4.167	-4.340	-4.725	-0.854	-0.870	-0.876	-0.875	-0.881
3.3	-4.005	-4.137	-4.302	-4.479	-4.885	-0.885	-0.900	-0.900	-0.902	-0.905
3.4	-4.113	-4.253	-4.435	-4.613	-5.039	-0.917	-0.931	-0.924	-0.929	-0.930
3.5	-4.222	-4.367	-4.566	-4.745	-5.187	-0.948	-0.962	-0.949	-0.958	-0.958
3.6	-4.334	-4.480	-4.694	-4.875	-5.328	-0.978	-0.993	-0.978	-0.987	-0.988
3.7	-4.451	-4.594	-4.819	-5.002	-5.464	-1.007	-1.024	-1.008	-1.017	-1.020
3.8	-4.573	-4.710	-4.942	-5.128	-5.598	-1.033	-1.054	-1.040	-1.047	-1.053
3.9	-4.701	-4.828	-5.063	-5.253	-5.731	-1.058	-1.084	-1.073	-1.078	-1.086
4.0	-4.832	-4.950	-5.185	-5.379	-5.867	-1.081	-1.113	-1.107	-1.109	-1.117
4.1	-4.967	-5.076	-5.307	-5.507	-6.010	-1.103	-1.140	-1.139	-1.139	-1.147
4.2	-5.102	-5.209	-5.429	-5.637	-6.158	-1.125	-1.165	-1.171	-1.169	-1.175
4.3	-5.238	-5.348	-5.552	-5.765	-6.308	-1.147	-1.188	-1.203	-1.200	-1.201
4.4	-5.373	-5.495	-5.677	-5.891	-6.461	-1.169	-1.208	-1.233	-1.231	-1.227
4.5	-5.509	-5.649	-5.804	-6.017	-6.615	-1.190	-1.225	-1.262	-1.262	-1.252
4.6	-5.645	-5.810	-5.933	-6.145	-6.770	-1.212	-1.240	-1.288	-1.293	-1.274
4.7	-5.781	-5.976	-6.063	-6.275	-6.930	-1.234	-1.254	-1.312	-1.324	-1.294
4.8	-5.918	-6.146	-6.195	-6.408	-7.096	-1.255	-1.266	-1.336	-1.354	-1.311
4.9	-6.055	-6.317	-6.326	-6.543	-7.268	-1.276	-1.277	-1.360	-1.383	-1.325
5.0	-6.192	-6.489	-6.457	-6.680	-7.444	-1.297	-1.288	-1.385	-1.412	-1.338



**Table 5. Coefficients for linear relationship  
between  $-\log_{10}(p)$  and  $\hat{t}_p$  for  $\omega = .60$**

$\rho$	intercepts $\alpha(\rho)$					slopes $\beta(\rho)$				
	$\kappa$ 1/10	1/3	1/2	2/3	1	1/10	1/3	1/2	2/3	1
0.1	-0.467	-0.470	-0.436	-0.459	-0.483	-0.144	-0.139	-0.164	-0.155	-0.142
0.2	-0.580	-0.589	-0.558	-0.583	-0.602	-0.163	-0.158	-0.177	-0.170	-0.162
0.3	-0.694	-0.708	-0.681	-0.707	-0.723	-0.181	-0.176	-0.191	-0.185	-0.183
0.4	-0.810	-0.830	-0.806	-0.833	-0.850	-0.200	-0.196	-0.206	-0.202	-0.204
0.5	-0.927	-0.953	-0.933	-0.962	-0.983	-0.221	-0.216	-0.223	-0.220	-0.226
0.6	-1.048	-1.080	-1.064	-1.094	-1.125	-0.242	-0.238	-0.243	-0.242	-0.249
0.7	-1.172	-1.209	-1.198	-1.230	-1.275	-0.266	-0.262	-0.265	-0.266	-0.274
0.8	-1.300	-1.343	-1.336	-1.369	-1.433	-0.291	-0.288	-0.292	-0.293	-0.300
0.9	-1.431	-1.480	-1.477	-1.511	-1.597	-0.318	-0.315	-0.321	-0.324	-0.329
1.0	-1.567	-1.620	-1.621	-1.656	-1.767	-0.348	-0.345	-0.353	-0.357	-0.359
1.1	-1.706	-1.765	-1.770	-1.803	-1.940	-0.378	-0.376	-0.387	-0.393	-0.391
1.2	-1.848	-1.911	-1.921	-1.952	-2.114	-0.411	-0.409	-0.423	-0.430	-0.424
1.3	-1.993	-2.060	-2.075	-2.103	-2.288	-0.444	-0.444	-0.460	-0.469	-0.458
1.4	-2.141	-2.209	-2.232	-2.254	-2.463	-0.478	-0.479	-0.496	-0.509	-0.493
1.5	-2.290	-2.359	-2.391	-2.407	-2.639	-0.513	-0.516	-0.531	-0.548	-0.529
1.6	-2.440	-2.510	-2.552	-2.563	-2.813	-0.548	-0.553	-0.566	-0.587	-0.566
1.7	-2.590	-2.660	-2.714	-2.724	-2.986	-0.584	-0.590	-0.600	-0.625	-0.603
1.8	-2.739	-2.811	-2.877	-2.888	-3.157	-0.620	-0.628	-0.635	-0.662	-0.641
1.9	-2.889	-2.962	-3.040	-3.055	-3.329	-0.656	-0.665	-0.670	-0.697	-0.679
2.0	-3.039	-3.114	-3.203	-3.225	-3.500	-0.692	-0.702	-0.705	-0.731	-0.717
2.1	-3.189	-3.267	-3.366	-3.397	-3.671	-0.728	-0.739	-0.740	-0.765	-0.755
2.2	-3.340	-3.422	-3.528	-3.570	-3.841	-0.764	-0.775	-0.775	-0.797	-0.794
2.3	-3.491	-3.577	-3.690	-3.743	-4.014	-0.800	-0.811	-0.810	-0.830	-0.833
2.4	-3.641	-3.733	-3.852	-3.915	-4.187	-0.835	-0.847	-0.844	-0.863	-0.871
2.5	-3.792	-3.890	-4.012	-4.085	-4.358	-0.871	-0.882	-0.879	-0.897	-0.911
2.6	-3.944	-4.050	-4.170	-4.254	-4.523	-0.906	-0.916	-0.916	-0.930	-0.951
2.7	-4.095	-4.211	-4.326	-4.421	-4.683	-0.941	-0.950	-0.955	-0.965	-0.992
2.8	-4.247	-4.374	-4.481	-4.585	-4.837	-0.976	-0.983	-0.995	-1.000	-1.033
2.9	-4.399	-4.540	-4.636	-4.746	-4.987	-1.011	-1.016	-1.035	-1.036	-1.074
3.0	-4.550	-4.708	-4.791	-4.904	-5.135	-1.046	-1.048	-1.074	-1.074	-1.115
3.1	-4.701	-4.877	-4.948	-5.059	-5.286	-1.082	-1.079	-1.111	-1.112	-1.156
3.2	-4.852	-5.046	-5.107	-5.215	-5.442	-1.116	-1.110	-1.146	-1.150	-1.196
3.3	-5.007	-5.213	-5.269	-5.376	-5.606	-1.151	-1.142	-1.178	-1.187	-1.234
3.4	-5.164	-5.378	-5.433	-5.544	-5.779	-1.184	-1.175	-1.209	-1.221	-1.271
3.5	-5.321	-5.540	-5.597	-5.717	-5.962	-1.217	-1.208	-1.240	-1.254	-1.306
3.6	-5.476	-5.699	-5.759	-5.895	-6.152	-1.251	-1.243	-1.273	-1.286	-1.340
3.7	-5.631	-5.855	-5.921	-6.074	-6.345	-1.285	-1.278	-1.307	-1.317	-1.373
3.8	-5.784	-6.010	-6.083	-6.252	-6.536	-1.320	-1.314	-1.341	-1.349	-1.404
3.9	-5.937	-6.163	-6.246	-6.424	-6.724	-1.354	-1.350	-1.376	-1.383	-1.436
4.0	-6.089	-6.316	-6.409	-6.586	-6.911	-1.389	-1.386	-1.410	-1.420	-1.467
4.1	-6.239	-6.469	-6.573	-6.735	-7.099	-1.424	-1.421	-1.444	-1.462	-1.497
4.2	-6.388	-6.624	-6.738	-6.874	-7.290	-1.460	-1.456	-1.478	-1.507	-1.525
4.3	-6.533	-6.782	-6.902	-7.007	-7.486	-1.496	-1.490	-1.512	-1.554	-1.553
4.4	-6.676	-6.943	-7.066	-7.136	-7.688	-1.534	-1.522	-1.548	-1.602	-1.580
4.5	-6.815	-7.106	-7.230	-7.264	-7.900	-1.572	-1.554	-1.585	-1.651	-1.605
4.6	-6.951	-7.270	-7.394	-7.391	-8.120	-1.611	-1.585	-1.622	-1.699	-1.629
4.7	-7.084	-7.435	-7.560	-7.517	-8.344	-1.651	-1.616	-1.658	-1.749	-1.652
4.8	-7.217	-7.600	-7.729	-7.640	-8.562	-1.691	-1.648	-1.691	-1.799	-1.675
4.9	-7.348	-7.763	-7.901	-7.760	-8.773	-1.731	-1.680	-1.720	-1.851	-1.698
5.0	-7.479	-7.926	-8.075	-7.879	-8.980	-1.771	-1.712	-1.748	-1.904	-1.722

## 5.5 Example with Nonperpendicularity Variation

Here we illustrate the use of Tables 1-5 in a fictitious example. We assume that the common part thickness for the two parts is  $W = .5$ , that the nominal hole diameters are  $D_0 = .5$ , that the hole diameter range is  $b - a = .003$ . For the pin diameter we assume a nominal value  $d_0 = .5 - \eta$ , where the nominal clearance  $\eta$  is left open at this point. The pin diameter variation range is  $d - c = .001$ . The radial accuracy for hole centering is assumed to be  $r = .005$  and we assume a bound  $\bar{\alpha}^\circ = .5^\circ$  on the deviations from perpendicularity.

The above data lead to the following worst case tolerance clearance

$$\begin{aligned} w'_0 &= a - .01745 \bar{\alpha}^\circ W - d - 2r \\ &= (.5 - .0015) - (.01745 .5 .5) - (.5 - \eta - .0005) - (2 .005) \\ &= \eta - .01636. \end{aligned}$$

For this worst case clearance to be positive we need to aim for a nominal clearance  $\eta$  in excess of .01636. This nominal clearance can be achieved either by increasing  $D_0$  or by decreasing  $d_0$  or by a combination of both.

For the statistical tolerance treatment we proceed as in the previous example calculation with the added interpolation over  $\omega$ . Here we have  $\rho = (b - a)/r = .6$ ,  $\kappa = (d - c)/(b - a) = 1/3$ , and  $\omega = .005075 W \bar{\alpha}^\circ / (b - a) = .4229$ , which is bracketed by  $\omega_1 = .30$  and  $\omega_2 = .45$ . Again we aim for a nonassembly risk of  $p = .001$ . From Table 3 we read off under  $\kappa = 1/3$ ,  $\rho = .6$ , and  $\omega = .30$

$$\alpha(.6) = -.747 \quad \text{and} \quad \beta(.6) = -.192 \quad \text{and thus} \quad \hat{t}_{.001}(.6) = -.747 + 3 \times (-.192) = -1.323$$

and thus

$$m'_0 = \eta + .005 \times (-1.323) = \eta - .006615.$$

Similarly, for  $\omega = .45$  we have

$$\alpha(.6) = -.918 \quad \text{and} \quad \beta(.6) = -.206 \quad \text{and thus} \quad \hat{t}_{.001}(.6) = -.918 + 3 \times (-.206) = -1.536$$

and thus

$$m'_0 = \eta + .005 \times (-1.536) = \eta - .00768.$$

Interpolating between .006615 and .00768 we get the following statistically stacked clearance for  $\omega = .4229$

$$m'_0 = \eta - .00749,$$

where

$$.00749 = .006615 + (.4229 - .30) \frac{.00768 - .006615}{.45 - .30}.$$

To render  $m'_0$  the nominal hole to pin clearance  $\eta$  needs to exceed .00749. We note the the worst case required nominal clearance value of .01636 exceeds the statistically toleranced value of .00749 by 118%, which amounts to significant and unnecessary slack.

## Appendix A

Here we derive a mathematical expression for the pinning criterion  $P_{\max-\min}$  as it was formulated in the main body of this paper.

Consider as starting position the one portrayed in Figure 1, namely with hole centers 1 and 3 aligned. There we have  $X_1 < X_2$ . If we move part 2 to the right or left we can only reduce the maximum clearance diameter at holes 1 and 3, although initially it will stay the same, since one hole is contained within the other. At the same time such left or right motions of part 2 will affect the maximum clearance diameter at holes 2 and 4. For the situation in Figure 1, with  $X_1 < X_2$ , a right motion of part 2 can only reduce (or maintain, in case the holes are nested) the maximum clearance diameter at holes 2 and 4. Such a right motion will not get us any closer to finding the maximum of the minimum plays at the two hole pairs. Thus only left motions of part 2 should be considered in this case. The farthest we should go with such left motion is the distance  $|X_1 - X_2|$ , because then the hole centers 2 and 4 become aligned and at that point any further motion in that direction becomes detrimental as explained before. Therefore, beginning at the above starting position, we should look for a left motion with distance  $\ell$  somewhere between 0 and  $|X_1 - X_2|$ , to find the maximum of the minimum plays at both hole pairs. If  $X_1 > X_2$ , one will have to interchange “left” and “right” in the above discussion of motions. If  $X_1 = X_2$ , no motion is necessary. In that case the maximum of the minimum plays at the two hole pairs is

$$P_{\max-\min} = \min [\min (D_1, D_3) - d_1, \min (D_2, D_4) - d_2] \quad (7)$$

and there is no way to increase that absolute maximum by any motion.

Left motion from the starting position will leave holes 1 and 3 nested as long as that left motion distance is within  $[0, |D_3 - D_1|/2]$ . Similarly, holes 2 and 4 will become nested under left motions as long as that left motion distance is within

$$\left[ [|X_1 - X_2| - |D_4 - D_2|/2]^+, |X_1 - X_2| + |D_4 - D_2|/2 \right],$$

where  $[x]^+ = x$  is  $x \geq 0$  and  $[x]^+ = 0$  for  $x < 0$ . This is seen by first moving hole centers 2 and 4 into alignment by a  $|X_1 - X_2|$  left motion and then realizing that a  $\pm |D_4 - D_2|/2$  displacement will leave the holes 2 and 4 barely nested. The use of the  $[ ]^+$  function is to rule out negative left motions, which amount to right motions ruled out from further considerations. Since we don't consider left motions beyond  $|X_1 - X_2|$ , the operative interval for keeping holes 2 and 4 nested is

$$\left[ [|X_1 - X_2| - |D_4 - D_2|/2]^+, |X_1 - X_2| \right].$$

There are two cases to distinguish here. In the first, when

$$|D_3 - D_1|/2 \geq [|X_1 - X_2| - |D_4 - D_2|/2]^+,$$

any left motion distance within the interval

$$\left[ [|X_1 - X_2| - |D_4 - D_2|/2]^+, \min(|X_1 - X_2|, |D_3 - D_1|/2) \right]$$

will leave both hole pairs nested and  $P_{\max-\min}$  will be as in (7), i.e., the largest value one could possibly get.

In the other case, when

$$A = |D_3 - D_1|/2 < [|X_1 - X_2| - |D_4 - D_2|/2]^+ = |X_1 - X_2| - |D_4 - D_2|/2 = B, \quad (8)$$

both hole pairs will become overlapping as soon as the left motion distance  $\ell$  is in the range  $[A, B]$ . While the left motion distance is in this interval any play gained or lost at one overlapping hole pair is lost or gained at the other.

At the left motion distance  $A = |D_3 - D_1|/2$  the play at the left hole pair 1 and 3 is

$$P_L(A) = \min(D_1, D_3) - d_1$$

while at the right hole pair 2 and 4 the play is

$$P_R(A) = Q_2(\Delta_2) - d_2 \quad \text{with} \quad \Delta_2 = |X_1 - X_2| - A > \frac{|D_4 - D_2|}{2} \geq 0.$$

Note that the original misalignment at 2 and 4, namely  $|X_1 - X_2|$  is not completely corrected by the left motion amount  $A$ . This follows from the inequality (8), the case considered here. Using the identity (2) the above expression for  $P_R(A)$  has the following equivalent form:

$$\begin{aligned} P_R(A) &= \min\left(D_2, D_4, \frac{D_2 + D_4}{2} - |X_1 - X_2| + \frac{|D_3 - D_1|}{2}\right) - d_2 \\ &= \min\left(D_2, D_4, \min(D_2, D_4) - |X_1 - X_2| + \frac{|D_3 - D_1|}{2} + \frac{|D_4 - D_2|}{2}\right) - d_2 \\ &= \min(D_2, D_4) - d_2 - \left(|X_1 - X_2| - \frac{|D_3 - D_1|}{2} - \frac{|D_4 - D_2|}{2}\right). \end{aligned}$$

At the left motion distance  $B = |X_1 - X_2| - |D_4 - D_2|/2$  we have

$$\Delta_2 = |X_1 - X_2| - B = |D_4 - D_2|/2 \quad \text{and} \quad Q_2(\Delta_2) = \min(D_2, D_4)$$

and thus the play at the holes 2 and 4 is

$$P_R(B) = \min(D_2, D_4) - d_2.$$

With respect to the left hole pair 1 and 3 we have under the same motion  $\Delta_1 = B$  and

$$\begin{aligned} Q_1(\Delta_1) &= \min\left(D_1, D_3, \frac{D_1 + D_3}{2} - \Delta_1\right) \\ &= \min\left(D_1, D_3, \frac{D_1 + D_3}{2} - |X_1 - X_2| + \frac{|D_4 - D_2|}{2}\right) \\ &= \min\left(D_1, D_3, \min(D_1, D_3) - |X_1 - X_2| + \frac{|D_4 - D_2|}{2} + \frac{|D_3 - D_1|}{2}\right) \\ &= \min(D_1, D_3) - \left(|X_1 - X_2| - \frac{|D_4 - D_2|}{2} - \frac{|D_3 - D_1|}{2}\right) \end{aligned}$$

Thus the play at the left hole pair 1 and 3 under this left  $B$  shift is

$$\begin{aligned} P_L(B) &= Q_1(\Delta_1) - d_1 \\ &= \min(D_1, D_3) - d_1 - \left( |X_1 - X_2| - \frac{|D_4 - D_2|}{2} - \frac{|D_3 - D_1|}{2} \right). \end{aligned}$$

As the amount  $\ell$  of left shift ranges from  $A$  to  $B$  the plays  $P_L(\ell)$  and  $P_R(\ell)$  at the left and right hole pairs have the form

$$P_L(\ell) = (A - \ell) + P_L(A) \quad \text{and} \quad P_R(\ell) = (\ell - B) + P_R(B)$$

with constant sum

$$P_L(\ell) + P_R(\ell) = A - B + P_L(A) + P_R(B).$$

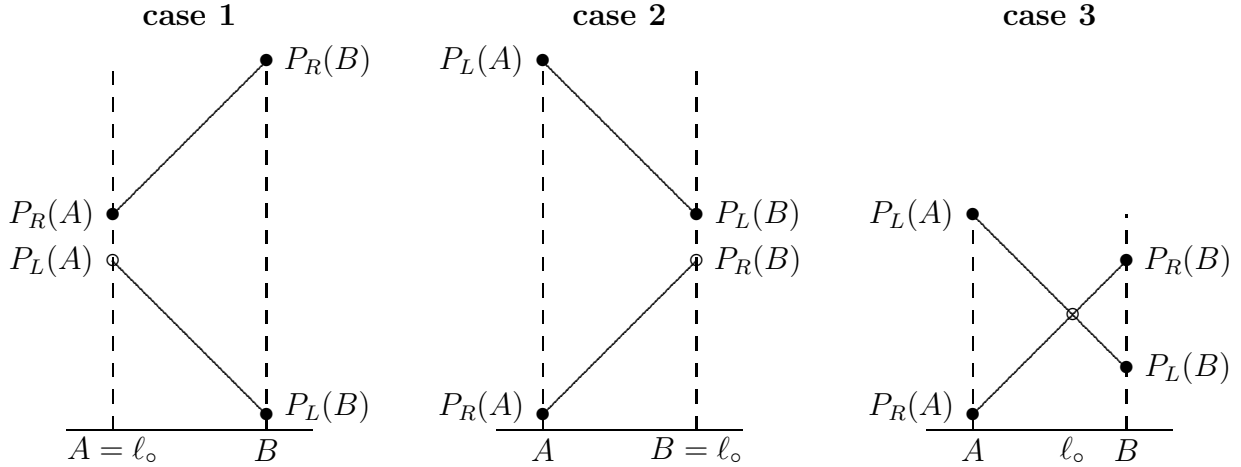


**Figure 12. Three cases**

There are basically three cases one needs to distinguish in order to find the  $\ell \in [A, B]$  that maximizes the minimum play at both hole pairs. These cases are illustrated in Figure 12, where the ordinate of  $\circ$  indicates the maximum of the minimum play in each case. In case 1, when  $P_R(A) > P_L(A)$  we should take  $\ell_0 = A$  and get as maximal minimum play  $P_L(A)$ . In case 2,  $P_R(B) < P_L(B)$ , we should take  $\ell_0 = B$  and get as maximal minimum play  $P_R(B)$ . In case 3, when  $P_L(A) \geq P_R(A)$  and  $P_L(B) \leq P_R(B)$  we should take

$$\ell_0 = \frac{A + B + P_L(A) - P_R(B)}{2}$$

and get as maximal minimum play

$$P_L(\ell_0) = P_R(\ell_0) = \frac{P_L(A) + P_R(A)}{2} = \frac{P_L(B) + P_R(B)}{2}.$$

Note that  $P_L(A) \geq P_R(A)$  and  $P_L(B) \leq P_R(B)$  is equivalent to

$$|\min(D_2, D_4) - d_2 - [\min(D_1, D_3) - d_1]| \leq |X_1 - X_2| - \frac{|D_3 - D_1| + |D_4 - D_2|}{2} \quad (9)$$

The above derivations for the maximal minimum play  $P_{\max-\min}$  can now be summarized as follows into four mutually exclusive and exhaustive cases of which the last three can be further combined into one, leaving us with two cases I and II which can then be combined in a single case.

**Case I:**

$$\begin{aligned} (9) \quad \implies \quad P_{\max-\min} &= \frac{\min(D_1, D_3) - d_1 + \min(D_2, D_4) - d_2}{2} \\ &\quad - \frac{1}{2} \left( |X_1 - X_2| - \frac{|D_3 - D_1| + |D_4 - D_2|}{2} \right) \\ &= \frac{D_1 + D_2 + D_3 + D_4}{4} - \frac{d_1 + d_2}{2} - \frac{|X_1 - X_2|}{2}, \end{aligned}$$

where the last simplification follows from identity (2). From (9) and the first form of  $P_{\max-\min}$  given in this case it follows that

$$P_{\max-\min} \leq \min [\min(D_1, D_3) - d_1, \min(D_2, D_4) - d_2] .$$

**Case a:**

$$(|D_3 - D_1| + |D_4 - D_2|)/2 \geq |X_1 - X_2|$$

$$\implies \quad P_{\max-\min} = \min [\min(D_1, D_3) - d_1, \min(D_2, D_4) - d_2]$$

**Case b:**

$$\min(D_2, D_4) - d_2 - [\min(D_1, D_3) - d_1] > |X_1 - X_2| - \frac{|D_3 - D_1| + |D_4 - D_2|}{2} > 0$$

$$\implies \quad P_{\max-\min} = \min(D_1, D_3) - d_1 = \min [\min(D_1, D_3) - d_1, \min(D_2, D_4) - d_2] .$$

**Case c:**

$$\min(D_2, D_4) - d_2 - [\min(D_1, D_3) - d_1] < - \left( |X_1 - X_2| - \frac{|D_3 - D_1| + |D_4 - D_2|}{2} \right) < 0$$

$$\implies P_{\max-\min} = \min(D_2, D_4) - d_2 = \min[\min(D_1, D_3) - d_1, \min(D_2, D_4) - d_2].$$

We can combine Cases a-c to

**Case II:**

$$|\min(D_2, D_4) - d_2 - [\min(D_1, D_3) - d_1]| > |X_1 - X_2| - \frac{|D_3 - D_1| + |D_4 - D_2|}{2}$$

$$\begin{aligned} \implies P_{\max-\min} &= \min[\min(D_1, D_3) - d_1, \min(D_2, D_4) - d_2] \\ &= \min\left(\frac{D_1 + D_3}{2} - \frac{|D_1 - D_3|}{2} - d_1, \frac{D_2 + D_4}{2} - \frac{|D_2 - D_4|}{2} - d_2\right) \\ &= \frac{D_1 + D_2 + D_3 + D_4}{4} - \frac{d_1 + d_2}{2} - \frac{|D_1 - D_3| + |D_2 - D_4|}{4} \\ &\quad - \left| \frac{D_1 - D_2 + D_3 - D_4 - 2(d_1 - d_2) - (|D_1 - D_3| - |D_2 - D_4|)}{4} \right| \\ &= \frac{D_1 + D_2 + D_3 + D_4}{4} - \frac{d_1 + d_2}{2} - \frac{|D_1 - D_3| + |D_2 - D_4|}{4} \\ &\quad - \frac{1}{2} |\min(D_1, D_3) - d_1 - [\min(D_2, D_4) - d_2]| \end{aligned}$$

after fivefold application of identity (2). Thus we can combine cases I and II to

$$\begin{aligned} P_{\max-\min} &= \frac{D_1 + D_2 + D_3 + D_4}{4} - \frac{d_1 + d_2}{2} \\ &\quad - \frac{1}{2} \max\left(|X_1 - X_2|, \frac{|D_1 - D_3| + |D_2 - D_4|}{2}\right. \\ &\quad \left. + |\min(D_1, D_3) - d_1 - [\min(D_2, D_4) - d_2]| \right) \end{aligned}$$

$$\begin{aligned}
&= \frac{|D_1 - D_3| + |D_2 - D_4|}{4} + \frac{\min(D_1, D_3) + \min(D_2, D_4)}{2} - \frac{d_1 + d_2}{2} \\
&\quad - \frac{1}{2} \max \left( |X_1 - X_2|, \frac{|D_1 - D_3| + |D_2 - D_4|}{2} \right. \\
&\qquad \qquad \qquad \left. + |\min(D_1, D_3) - d_1 - [\min(D_2, D_4) - d_2]| \right).
\end{aligned}$$



## Appendix B

Here we determine the diameter of the largest circle fitting into the intersection of two ellipses  $\mathcal{E}_1$  and  $\mathcal{E}_2$  of same shape and size, aligned but offset from each other along their major axis, see Figure 10 for two generic cases.

Because of the rotational and translational symmetry of the problem formulation we may, without loss of generality, assume that the common major axis of these two ellipses coincides with the  $x$ -axis and that their perimeter curves  $\partial\mathcal{E}_1$  and  $\partial\mathcal{E}_2$  are given as the set of points  $(x, y)$  satisfying the following two equations:

$$\partial\mathcal{E}_1 : \frac{y^2}{b^2} + \frac{(x - \Delta)^2}{a^2} = 1 \quad \text{and} \quad \partial\mathcal{E}_2 : \frac{y^2}{b^2} + \frac{(x + \Delta)^2}{a^2} = 1 \quad \text{with } \Delta \geq 0.$$

The major axis being along the  $x$ -axis entails that  $b \leq a$ . In fact, we will assume  $b < a$ , because when  $a = b$  we deal with two circles and it is easily seen that the largest inscribed circle has radius  $r = a - \Delta$ , provided  $a \geq \Delta$ . If the latter is not the case, no such circle exists, although we will still speak of a ‘‘circle’’ with negative radius  $r$ . In a way that negative radius expresses how far away we are from a situation with a real inscribed circle.

From symmetry considerations it follows that the biggest circle within  $\mathcal{E}_1 \cap \mathcal{E}_2$  is centered at  $(0, 0)$  and all normals at points where one of the ellipses and the inscribed circle touch each other have to pass through the origin.

The equation of the line through a point  $(x_0, y_0)$  on  $\partial\mathcal{E}_1$  which is tangent to  $\partial\mathcal{E}_1$  is given by:

$$\frac{(x - \Delta)(x_0 - \Delta)}{a^2} + \frac{yy_0}{b^2} = 1 \quad \text{with} \quad \frac{y_0^2}{b^2} + \frac{(x_0 - \Delta)^2}{a^2} = 1$$

and the equation of the line through a point  $(x_0, y_0)$  on  $\partial\mathcal{E}_1$  which is normal to  $\partial\mathcal{E}_1$  derives from that as:

$$y = \frac{y_0}{x_0 - \Delta} \frac{a^2}{b^2} (x - x_0) + y_0 \quad \text{with} \quad \frac{y_0^2}{b^2} + \frac{(x_0 - \Delta)^2}{a^2} = 1.$$

The above requires that  $x_0 \neq \Delta$ . The case of  $x_0 = \Delta$  is of no interest here, since it concerns a line parallel to the  $y$ -axis but not passing through the origin. Above the origin was identified as the center of the inscribed maximal circle. In saying that this line does not pass through the origin we assume that  $\Delta > 0$ . When  $\Delta = 0$  we are faced with two coinciding ellipses and the radius of the maximally inscribed circle is  $r = b$  in that case.

The above requirement that normals through common tangent points  $(x_0, y_0)$  on ellipse  $\partial\mathcal{E}_1$  and inscribed circle pass through the origin translates to

$$0 = \frac{y_0}{x_0 - \Delta} \frac{a^2}{b^2} (-x_0) + y_0 \quad \text{and} \quad \frac{y_0^2}{b^2} + \frac{(x_0 - \Delta)^2}{a^2} = 1. \quad (10)$$

When  $y_0 \neq 0$  the first of the equations in (10) is equivalent to

$$x_0 - \Delta = x_0 a^2/b^2 \quad \text{or} \quad x_0 = \frac{\Delta}{1 - a^2/b^2} \quad (< 0).$$

The two equations in (10) combine to

$$\frac{y_0^2}{b^2} + \frac{x_0^2 a^4}{a^2 b^4} = 1 \quad \text{or} \quad b^2 \left[ 1 - \frac{a^2 \Delta^2}{(b^2 - a^2)^2} \right] = y_0^2.$$

Thus, if

$$1 - \frac{a^2 \Delta^2}{(b^2 - a^2)^2} > 0, \quad (11)$$

there are two solutions to the equations (10) and therefore two points at which the inscribed circle touches  $\partial\mathcal{E}_1$ , and similarly two points at which the inscribed circle touches  $\partial\mathcal{E}_2$ , see the left example in Figure 10. This circle has radius

$$r = \sqrt{\frac{\Delta^2}{(1 - a^2/b^2)^2} + b^2 \left[ 1 - \frac{a^2 \Delta^2}{(b^2 - a^2)^2} \right]} = b \sqrt{1 - \frac{\Delta^2}{a^2 - b^2}}.$$

When  $a \geq b$  the main axis segment contained within  $\mathcal{E}_1 \cap \mathcal{E}_2$  has length  $2a - 2\Delta$ . A circle with radius  $r = a - \Delta \geq 0$  will go through  $(\pm r, 0)$  and touch both ellipses at  $(-r, 0)$  and  $(r, 0)$ , respectively, see the right example in Figure 10. However, this circle will only be an inscribed circle if its radius  $r$  is at most equal to the curvature  $R$  of these ellipses at these tangent points. According to Bronshtein and Semendyayev<sup>1</sup> (page 202) this curvature is  $R = b^2/a$ . Note that the condition

$$R = \frac{b^2}{a} \geq a - \Delta = r$$

is equivalent to

$$1 - \frac{a^2 \Delta^2}{(b^2 - a^2)^2} \leq 0,$$

which is complementary to the above case (11). To summarize the above, the maximal inscribed circle has radius

$$r = b \sqrt{1 - \frac{\Delta^2}{a^2 - b^2}} \quad \text{for } \Delta < a - b^2/a$$

and

$$= a - \Delta \quad \text{for } \Delta \geq a - b^2/a.$$

In the latter case we can have a negative radius, i.e., no real inscribed circle at all, when  $a < \Delta$ . For the reasons given above we leave negative radii as they are.

Note that the two special cases  $\Delta = 0$  and  $a = b$ , treated separately above, are included in this last summary form for  $r$ .

The general result above is now specialized to the case where the two ellipses are generated by the entry and exit contour of a cylinder of diameter  $D$  passing at some angle through a

---

<sup>1</sup>Bronshtein, I.N. and Semendyayev, K.A. (1985). *Handbook of Mathematics*.

plate of uniform thickness  $W$ , see Figure 13. As we project the centers of these two ellipses perpendicularly onto the entry plane their distance is denoted by  $2\Delta$ , linking it up with our previous notation in the general formulation. The special aspect is that the length  $2a$  of the major axis of either ellipse is linked here to this  $2\Delta$ , whereas  $2b = D$  for any  $\Delta$ .

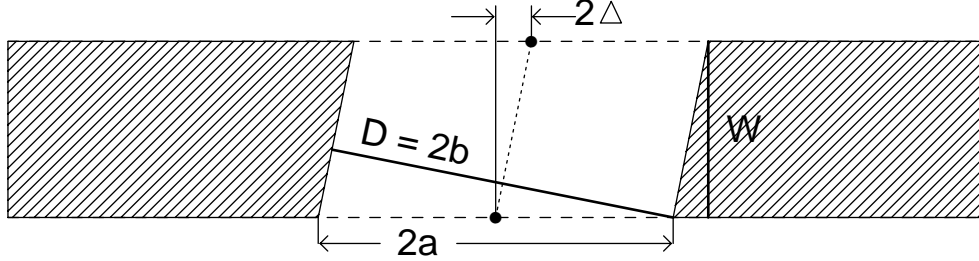


**Figure 13. Hole cross section**

From Figure 13 and the similarity of triangles we have the following relationship

$$\frac{2a}{D} = \frac{\sqrt{W^2 + 4\Delta^2}}{W} \quad \text{and thus} \quad a = \frac{D}{2} \sqrt{1 + \frac{4\Delta^2}{W^2}}.$$

From this and  $2b = D$  we have

$$a^2 - b^2 = \frac{D^2}{4} \left(1 + \frac{4\Delta^2}{W^2}\right) - \frac{D^2}{4} = \frac{D^2\Delta^2}{W^2}.$$

The condition  $\Delta < a - b^2/a$  becomes

$$\begin{aligned} a\Delta < a^2 - b^2 &= \frac{D^2\Delta^2}{W^2} & \text{or} & \quad \frac{D}{2} \sqrt{1 + \frac{4\Delta^2}{W^2}} < \frac{D^2\Delta}{W^2} \\ \text{or} \quad \sqrt{1 + \frac{4\Delta^2}{W^2}} &< \frac{2\Delta D}{W^2} & \text{or} & \quad 1 < \frac{4\Delta^2}{W^4} (D^2 - W^2). \end{aligned} \quad (12)$$

In the following we will distinguish two cases, namely Case I:  $D > W$  and Case II:  $D \leq W$ .

**Case I:** Condition (12) is equivalent to

$$2\Delta > \frac{W^2}{\sqrt{D^2 - W^2}}.$$

Under this condition the maximal cylinder, that can pass perpendicularly through the hole, has diameter

$$D' = D \sqrt{1 - \frac{\Delta^2}{a^2 - b^2}} = D \sqrt{1 - \frac{W^2}{D^2}} = \sqrt{D^2 - W^2} \quad (< D)$$

regardless of the actual value of  $\Delta$  satisfying  $2\Delta > W^2/\sqrt{D^2 - W^2}$ .

The complement of (12), i.e.,  $\Delta \geq a - b^2/a$ , is equivalent to

$$\frac{2\Delta}{W} \leq \frac{1}{\sqrt{D^2/W^2 - 1}}$$

in which case the maximal cylinder, that can pass perpendicularly through the hole, has diameter

$$D' = 2(a - \Delta) = D \sqrt{1 + \frac{4\Delta^2}{W^2}} - 2\Delta, \quad (13)$$

with  $D' \leq D$ , since

$$f(x) = D \sqrt{1 + x^2/W^2} - x \quad \text{is decreasing for } x = 2\Delta \in \left[0, \frac{W}{\sqrt{D^2/W^2 - 1}}\right].$$

**Case II:** Here condition (12) can not occur. Thus we only have to deal with  $\Delta \geq a - b^2/a$ , in which case the maximal cylinder, that can pass perpendicularly through the hole, again has diameter  $D'$  given by (13).

## Appendix C

This appendix contains the figures corresponding to Figures 6-7 for the values  $\kappa = 1/10, 1/3, 1/2, 2/3$ . Table 1 was derived from all these spline fits.

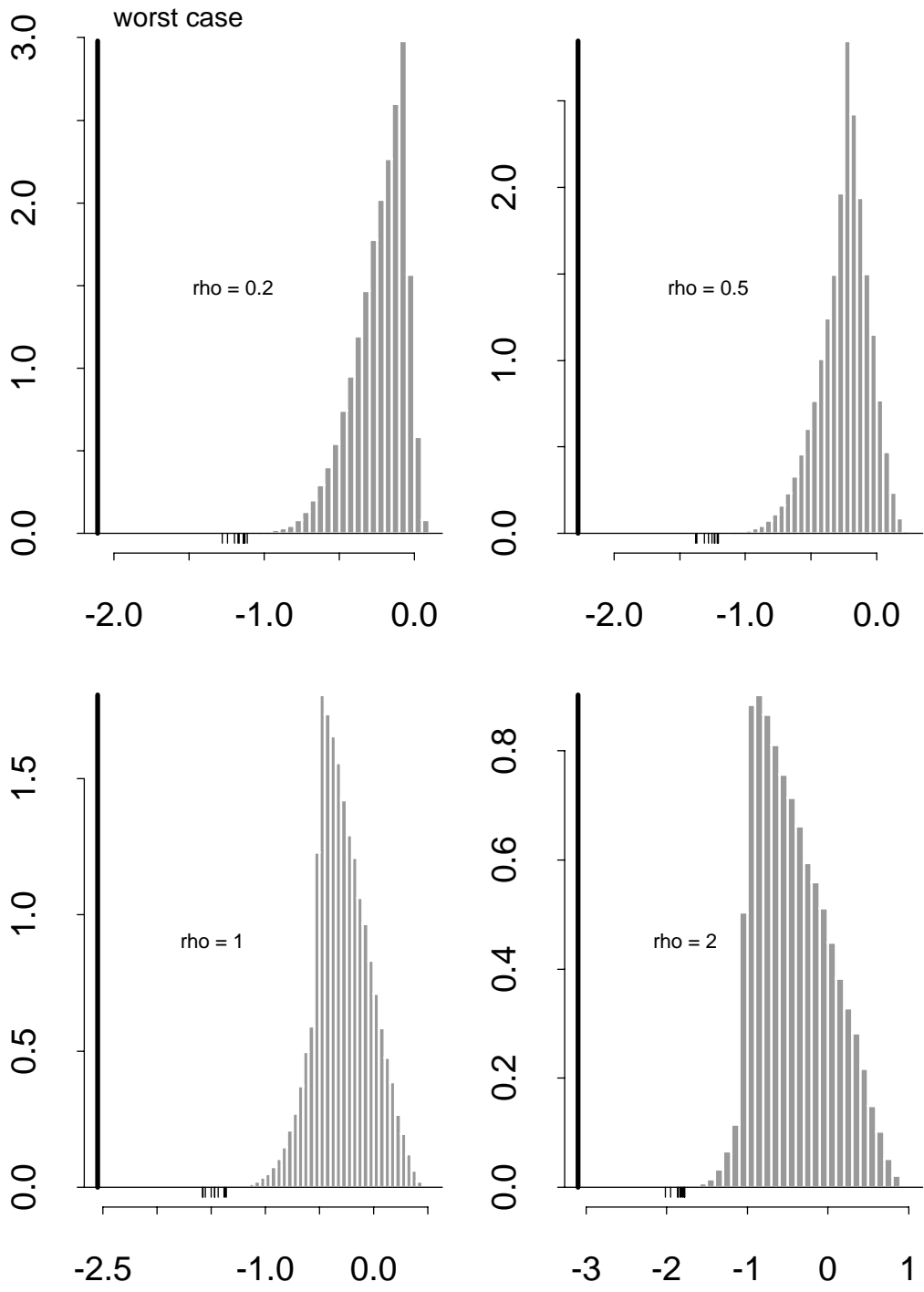


Figure 14. Simulated distributions of  $T$ , for  $\kappa = .1$ ,  $\rho = 1, 2, 3, 4$ , and 100,000 simulations

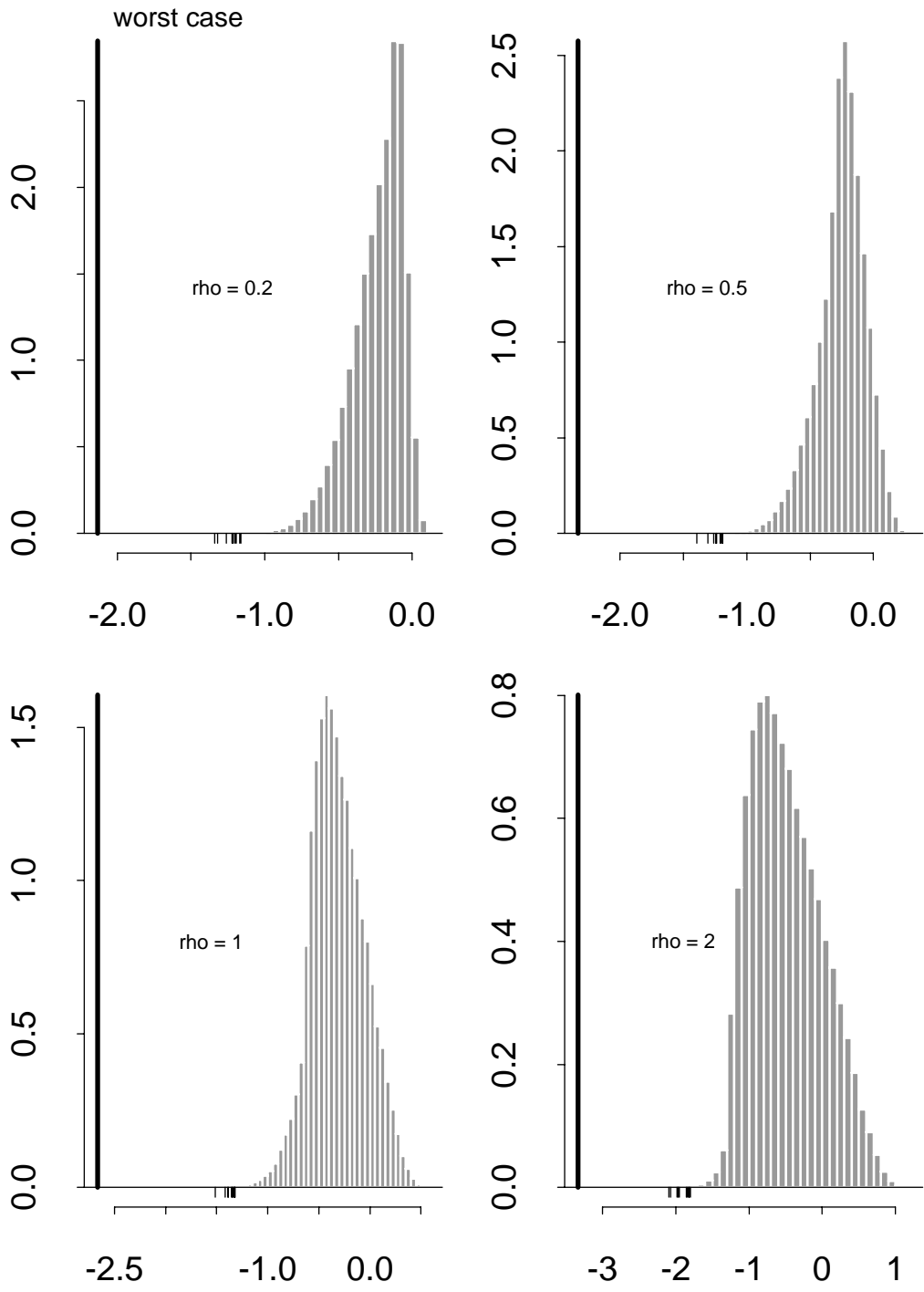


Figure 15. Simulated distributions of  $T$ , for  $\kappa = 1/3$ ,  $\rho = 1, 2, 3, 4$ , and 100,000 simulations

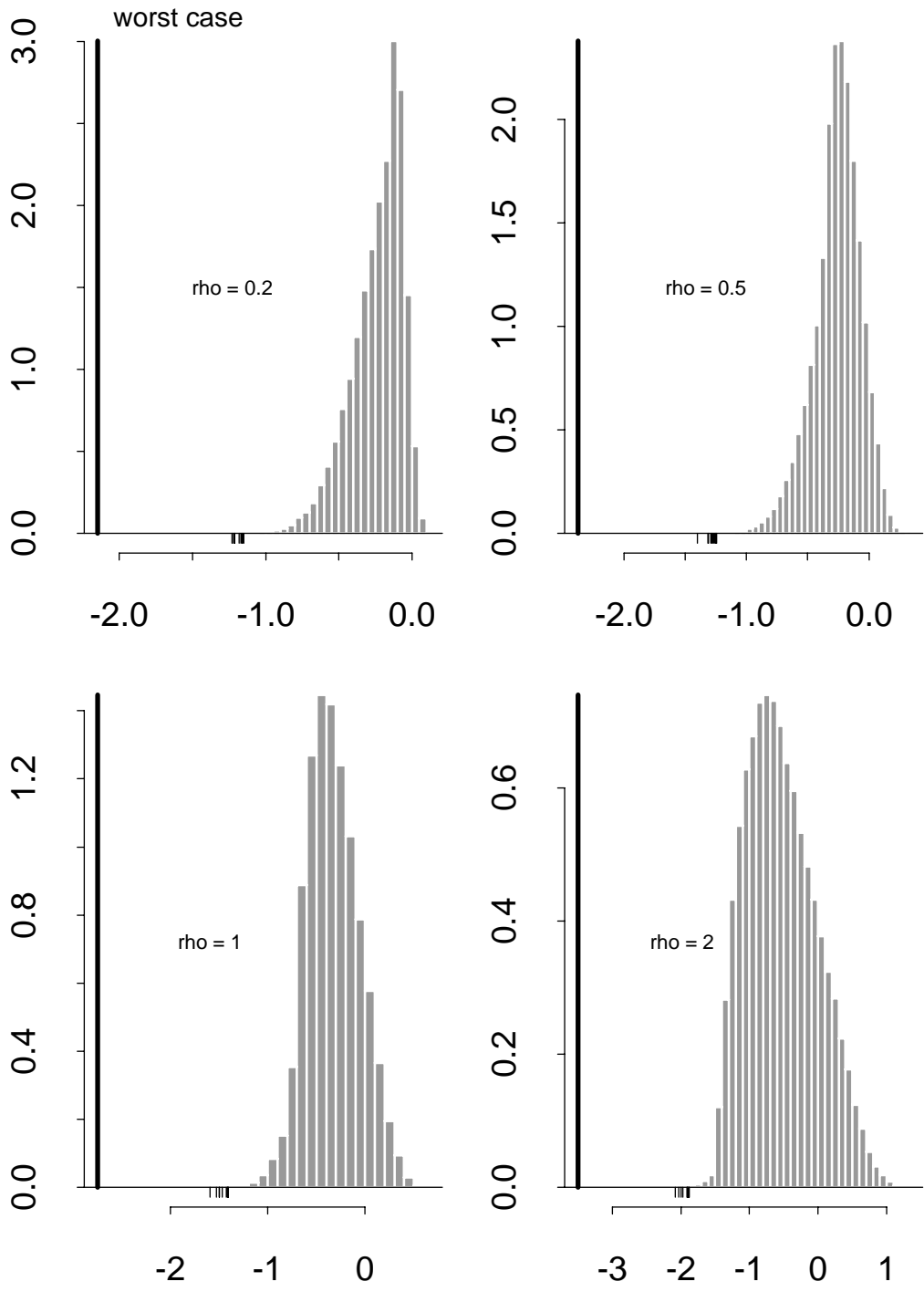


Figure 16. Simulated distributions of  $T$ , for  $\kappa = .5$ ,  
 $\rho = 1, 2, 3, 4$ , and 100,000 simulations



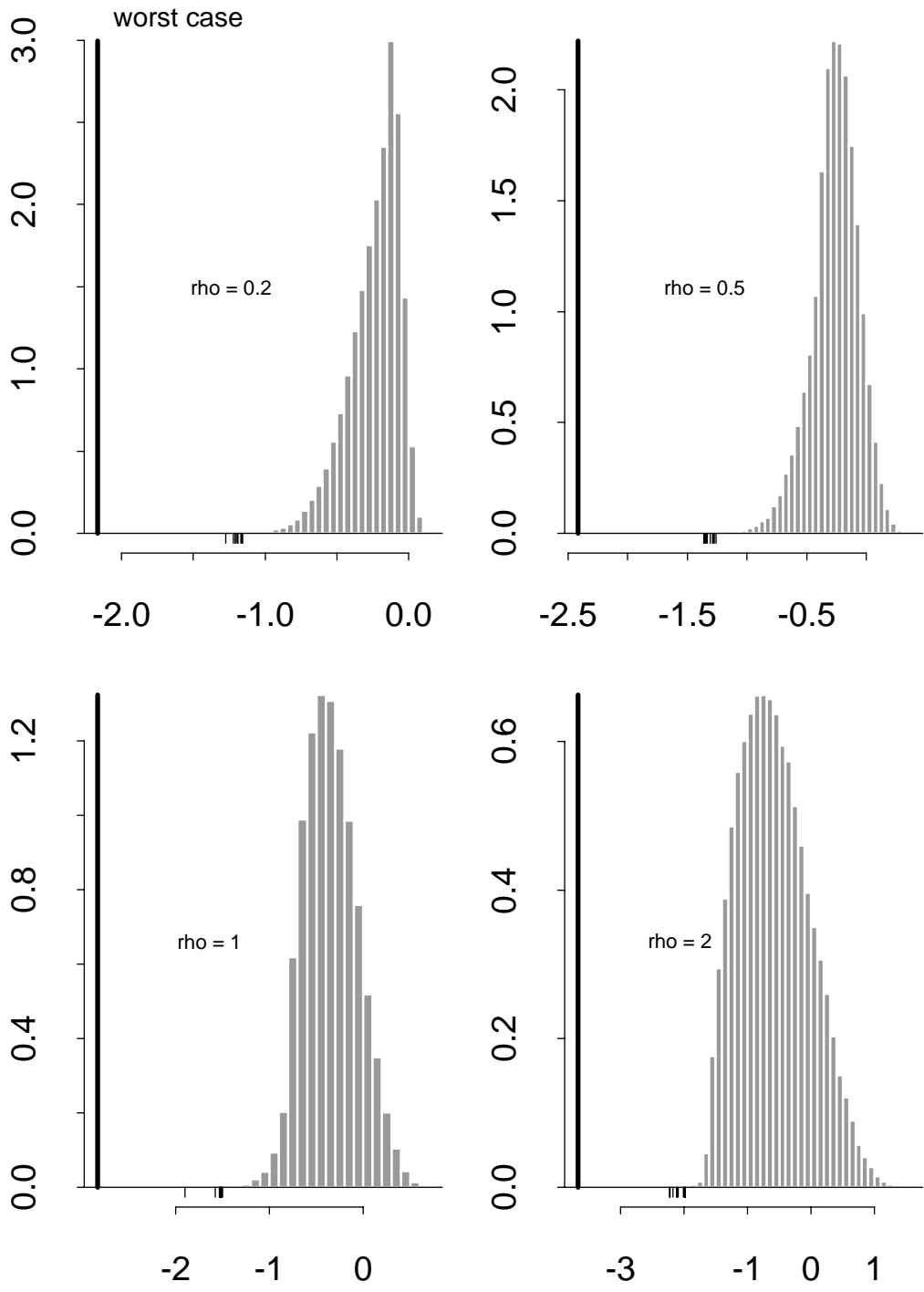


Figure 17. Simulated distributions of  $T$ , for  $\kappa = 2/3$ ,  $\rho = 1, 2, 3, 4$ , and 100,000 simulations

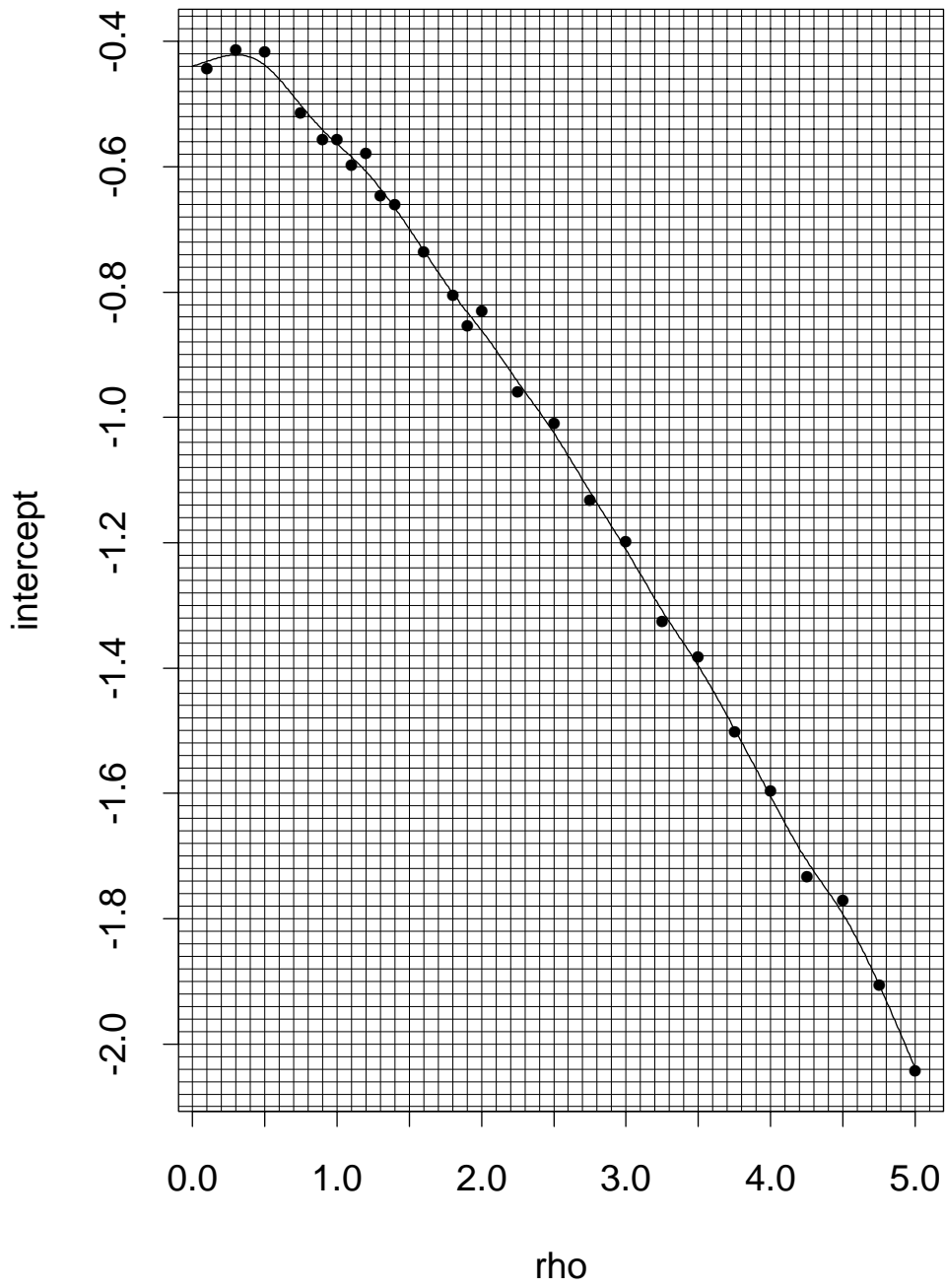


Figure 18. Average of 10 estimated intercepts for linear relationship between  $-\log_{10}(p)$  and  $\hat{t}_p$  for  $\kappa = .1$

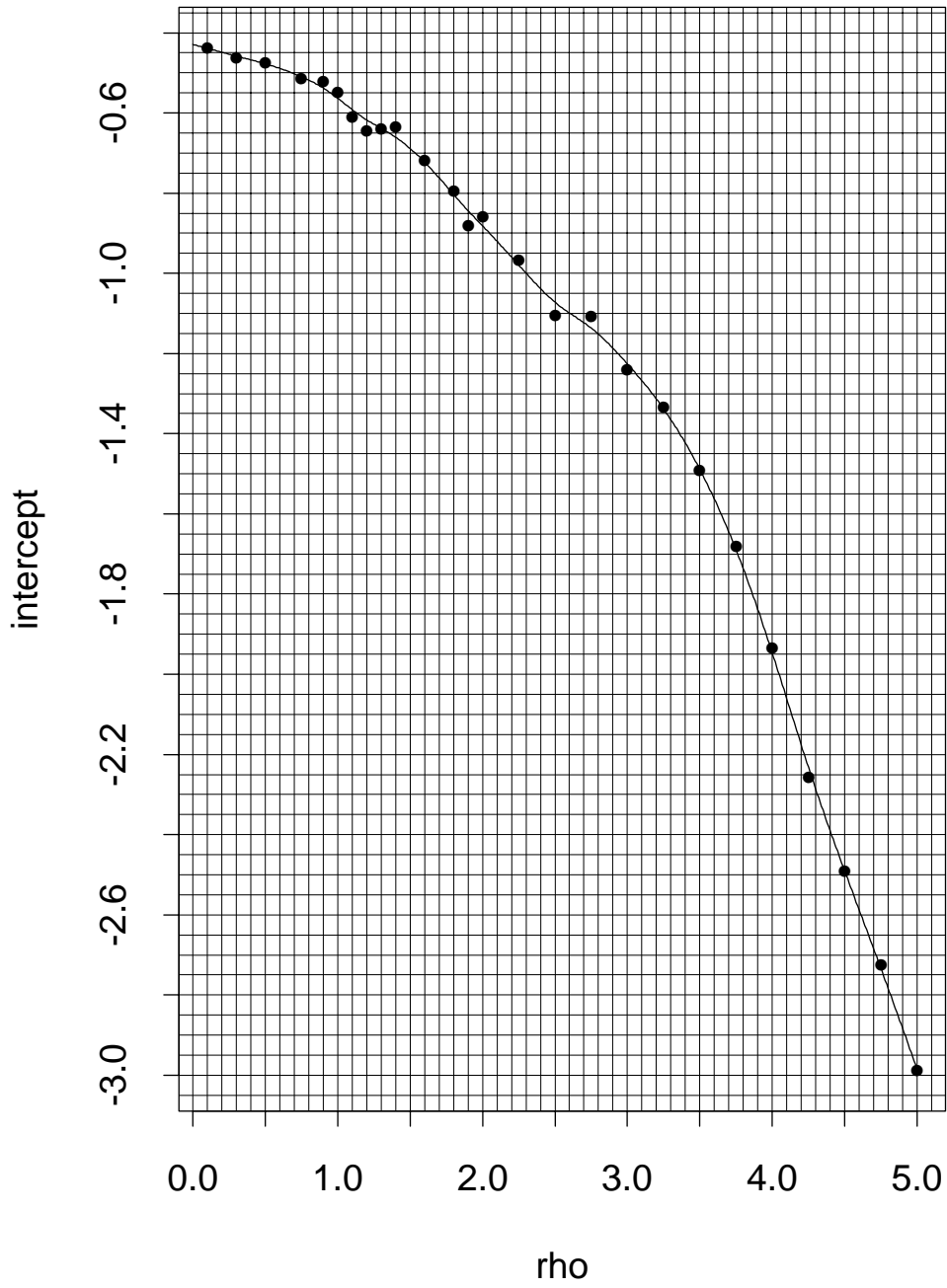


Figure 19. Average of 10 estimated intercepts for linear relationship between  $-\log_{10}(p)$  and  $\hat{t}_p$  for  $\kappa = 1/3$

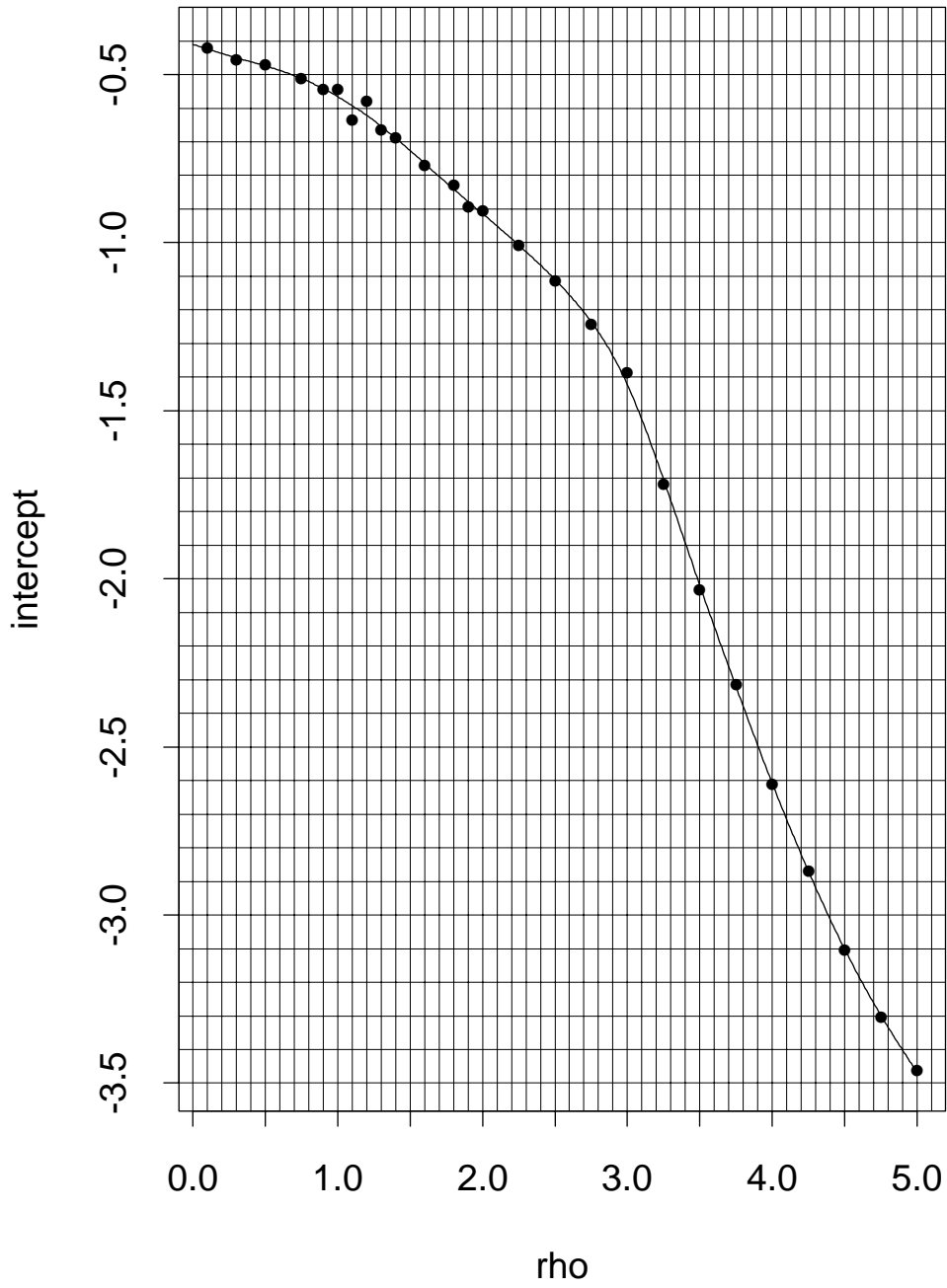


Figure 20. Average of 10 estimated intercepts for linear relationship between  $-\log_{10}(p)$  and  $\hat{t}_p$  for  $\kappa = .5$

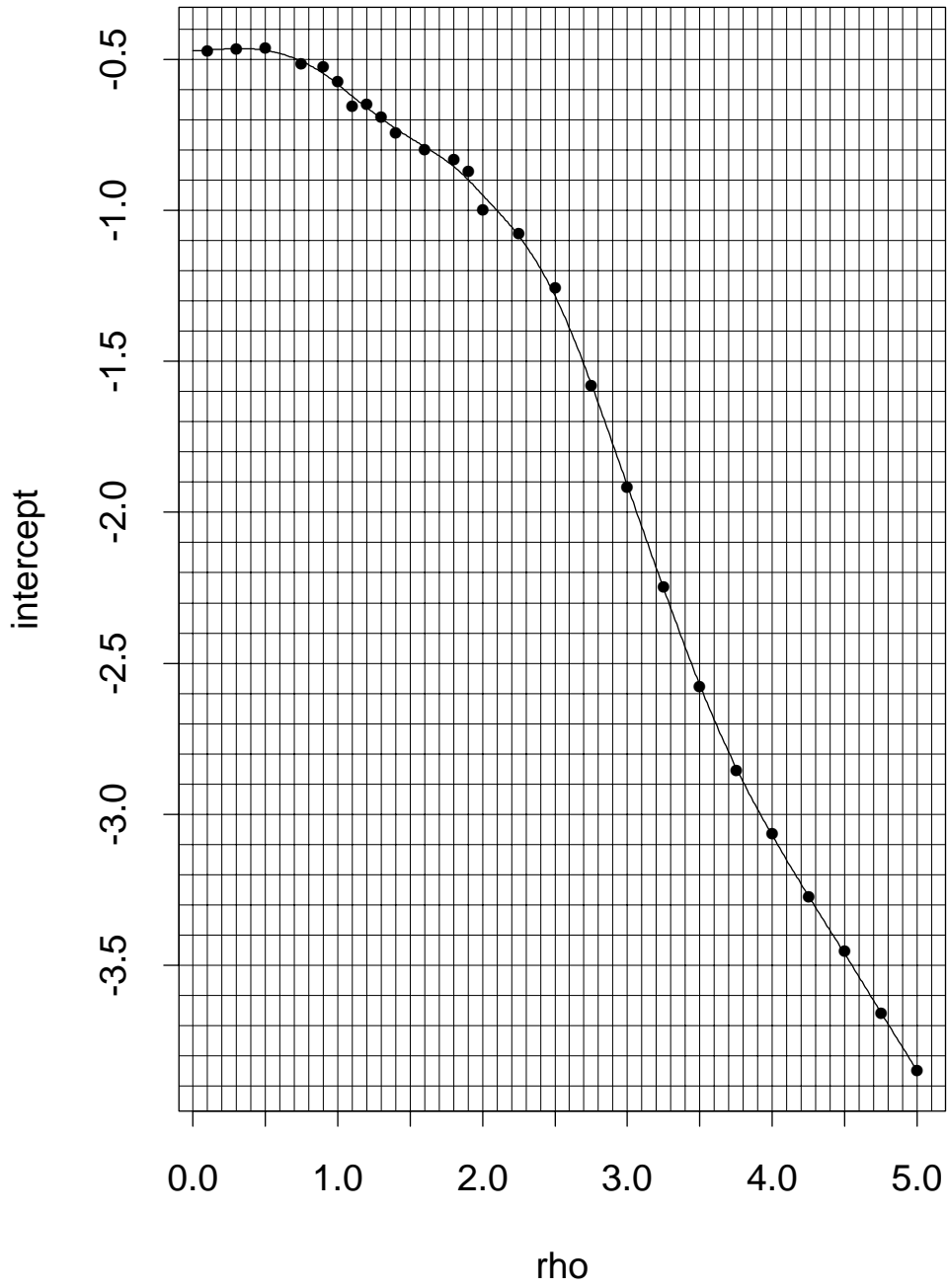


Figure 21. Average of 10 estimated intercepts for linear relationship between  $-\log_{10}(p)$  and  $\hat{t}_p$  for  $\kappa = 2/3$

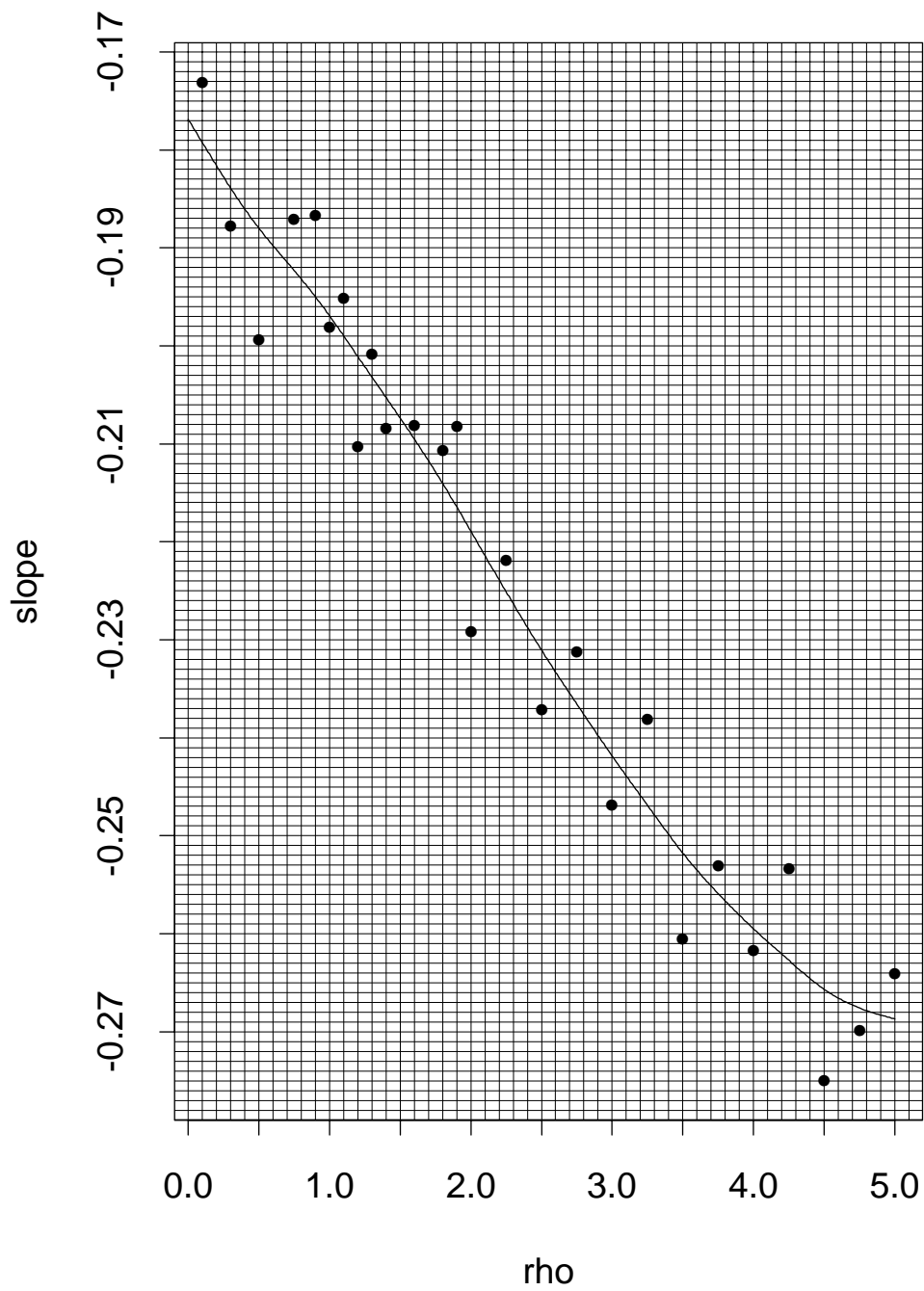


Figure 22. Average of 10 estimated slopes for linear relationship between  $-\log_{10}(p)$  and  $\hat{t}_p$  for  $\kappa = .1$

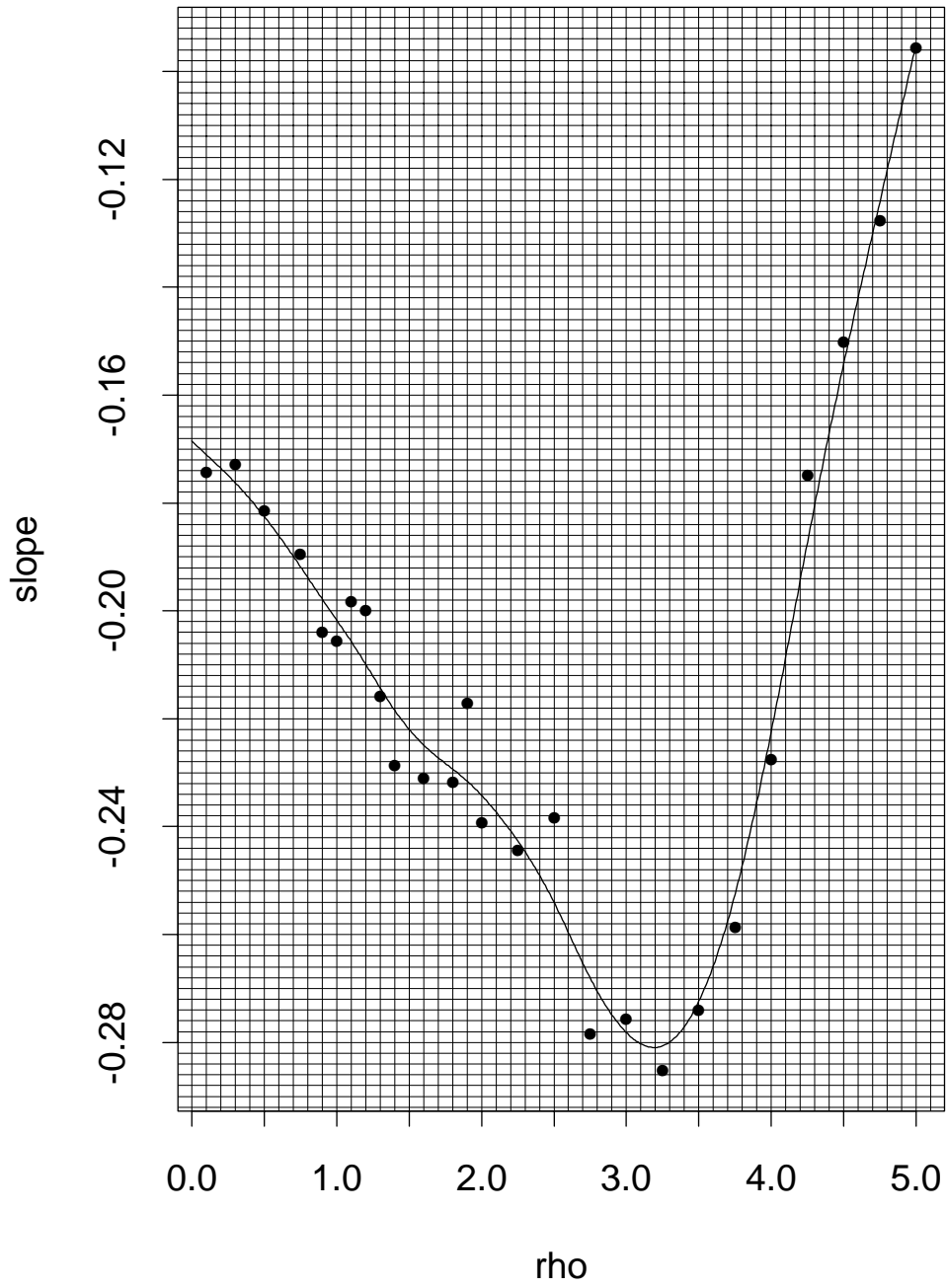


Figure 23. Average of 10 estimated slopes for linear relationship between  $-\log_{10}(p)$  and  $\hat{t}_p$  for  $\kappa = 1/3$

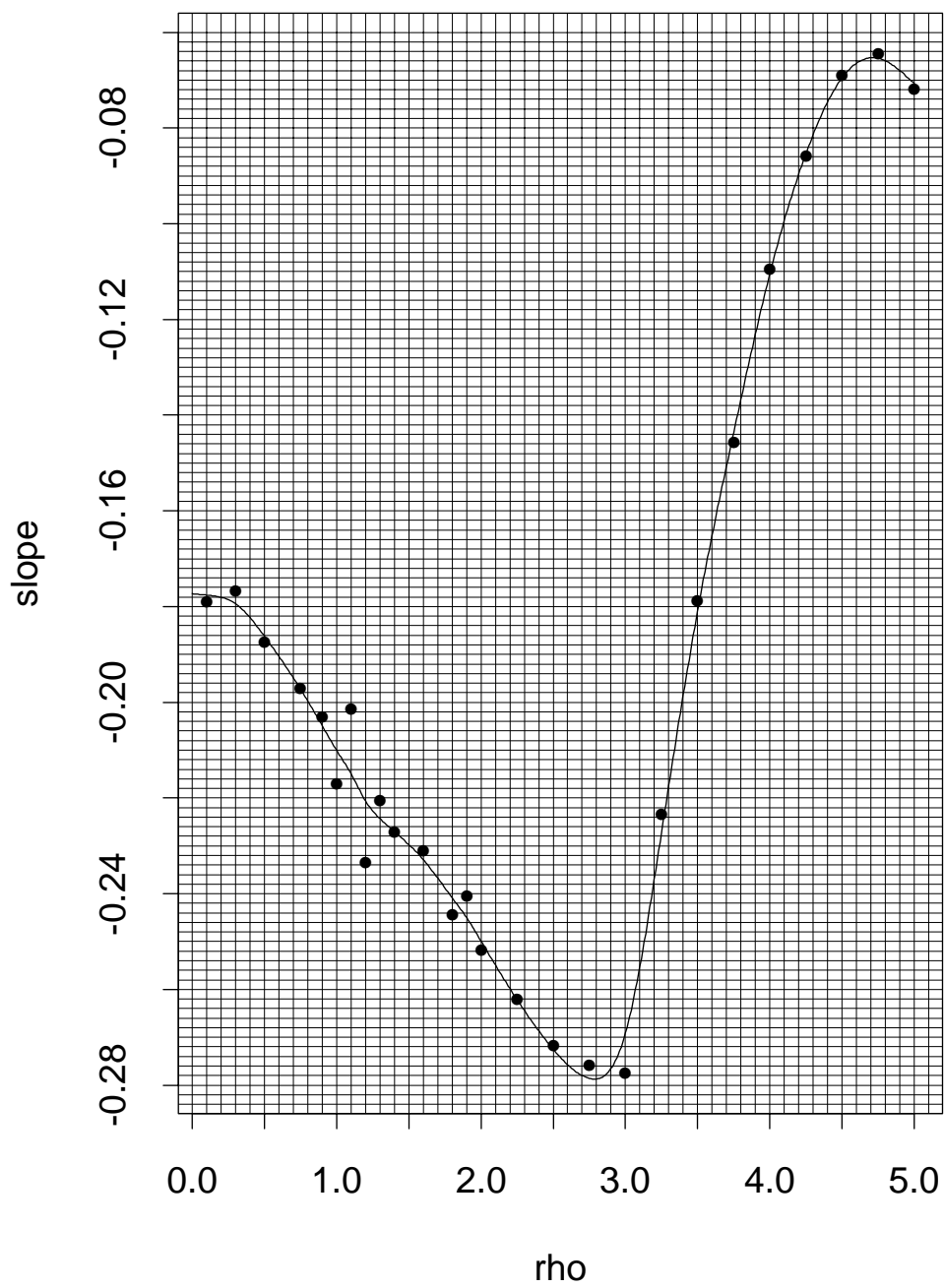


Figure 24. Average of 10 estimated slopes for linear relationship between  $-\log_{10}(p)$  and  $\hat{t}_p$  for  $\kappa = .5$



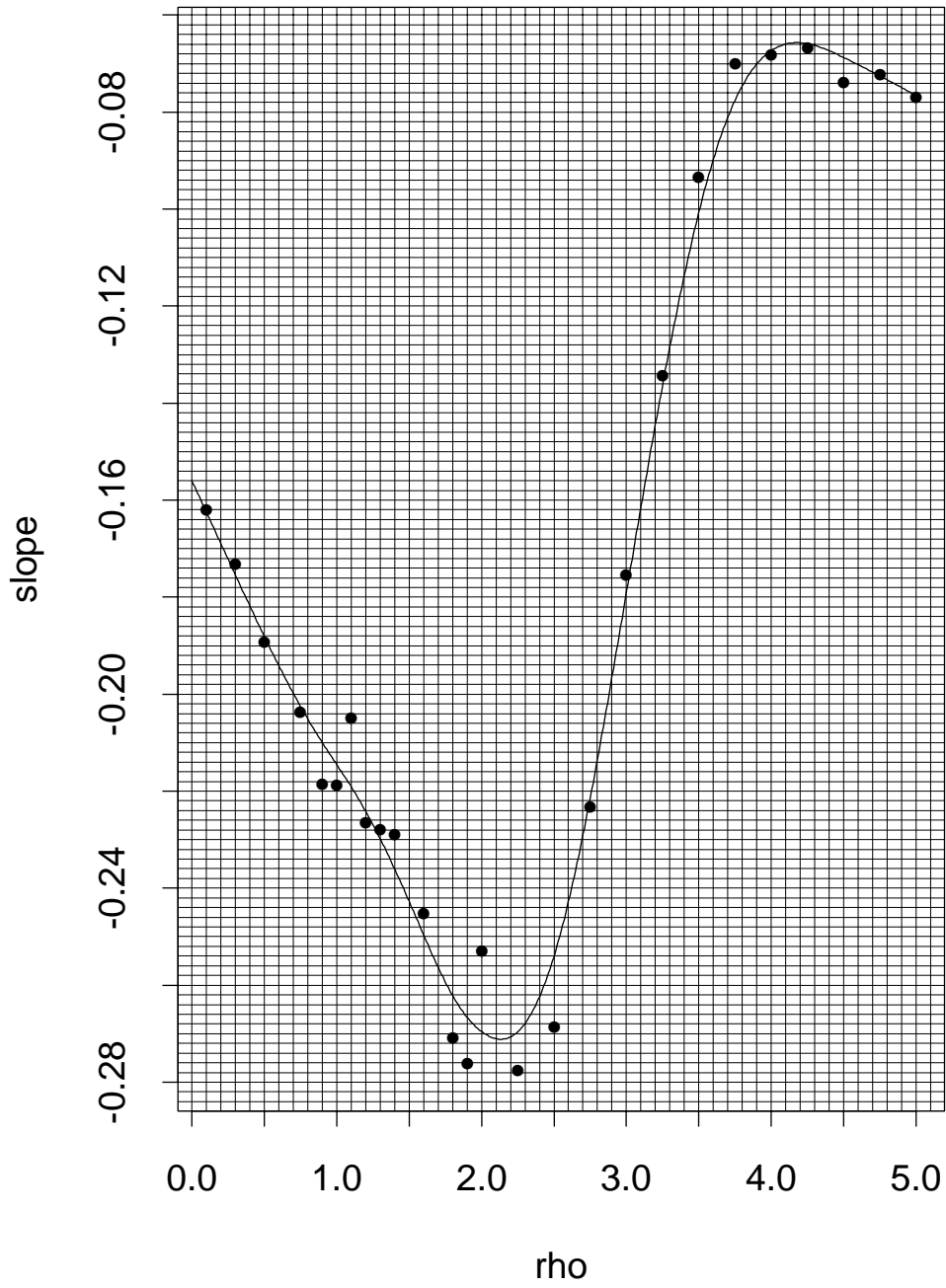


Figure 25. Average of 10 estimated slopes for linear relationship between  $-\log_{10}(p)$  and  $\hat{t}_p$  for  $\kappa = 2/3$